Temporally varying natural mortality: sensitivity of a virtual population analysis and an exploration of alternatives

Preprint of article accepted to Fisheries Research
http://dx.doi.org/10.1016/j.fishres.2016.09.002

Shanae D. Allen [a,b,1]
William H. Satterthwaite [b,*]
David G. Hankin [c]
Diana J. Cole [d]
Michael S. Mohr [b]

[a] University of California, Santa Cruz
Cooperative Institute for Marine Ecosystems and Climate (CIMEC)
Award number: NA15OAR 4320071
110 Shaffer Road
Santa Cruz, California 95060, USA

[b] Fisheries Ecology Division
Southwest Fisheries Science Center
National Marine Fisheries Service
National Oceanographic and Atmospheric Administration
110 Shaffer Road
Santa Cruz, California 95060, USA

[c] Department of Fisheries Biology
Humboldt State University
1 Harpst Street
Arcata, California 95521, USA

[d] School of Mathematics
Statistics and Actuarial Science
University of Kent
Canterbury, Kent, CT2 7NF, UK

[1] *Present address:*
Fish and Wildlife Research Institute
Florida Fish and Wildlife Conservation Commission
100 Eighth Avenue SE
St. Petersburg, Florida 33701, USA

[*] Corresponding author
E-mail address: will.satterthwaite@noaa.gov

Keywords:

1. age- and time-dependent models
2. virtual population analysis
3. cohort reconstruction
4. natural mortality
5. salmon stock assessment

Highlights:

1. Salmon cohort reconstructions (CR) commonly assume fixed, low adult natural mortality rate.
2. CR estimate remaining vital rates well unless adult natural mortality rate is approximately twice that assumed.
3. Separable models make adult natural mortality rate identifiable through additive effects.
4. Separable models did not outperform CR and performed worse when assumptions violated.
5. Some separable models estimated adult natural mortality rates with little bias under conditions conducive to CR.

1 Abstract

Cohort reconstructions (CR) currently applied in Pacific salmon management estimate temporally variant exploitation, maturation, and juvenile natural mortality rates but require an assumed (typically invariant) adult natural mortality rate (d_A), resulting in unknown biases in the remaining vital rates. We explored the sensitivity of CR results to misspecification of the mean and/or variability of d_A, as well as the potential to estimate d_A directly using models that assumed separable year and age/cohort effects on vital rates (Separable Cohort Reconstruction, SCR). For CR, given the commonly assumed $d_A = 0.2$, the error (RMSE) in estimated vital rates is generally small (≤ 0.05) when annual values of d_A are low to moderate (≤ 0.4). The greatest absolute errors are in maturation rates, with large relative error in the juvenile survival rate. The ability of CR estimates to track temporal trends in the juvenile natural mortality rate is adequate (Pearson's correlation coefficient > 0.75) except for high d_A (≥ 0.6) and high variability (CV > 0.35). The alternative SCR models allowing estimation of time-varying d_A by assuming additive effects in natural mortality, fishing mortality, and/or maturation rates did not outperform CR across all simulated scenarios, and are less accurate when additivity assumptions are violated. Nevertheless an SCR model assuming additive effects on fishing and natural (juvenile and adult) mortality rates led to nearly unbiased estimates of all quantities estimated using CR, along with borderline acceptable estimates of the mean d_A under multiple sets of conditions conducive to CR. Adding an assumption of additive effects on the maturation rates allowed nearly unbiased estimates of the mean d_A as well. The SCR models performed slightly better than CR when the vital rates covaried as assumed. These separable models could serve as a partial check on the validity of CR assumptions about the adult natural mortality rate, or even a preferred alternative if there is strong reason to believe the vital rates, including juvenile and adult natural mortality rates, covary strongly across years or age classes as assumed.

2 Introduction

Fisheries stock assessments use a variety of statistical and mathematical tools in an attempt to understand the current abundance and dynamics of fished stocks. While the form of model employed in a stock assessment may vary considerably depending on scientific and management context, estimates of natural morality are an integral component of stock assessment. It is known that many results from stock assessments can be heavily influenced by the choice of natural mortality (e.g., biological reference points, Goodyear, 1993). Yet, owing to the difficulty of directly estimating natural mortality, fixed external estimates or assumed values are frequently used. Temporal and/or age-dependent variation in natural mortality undoubtedly exists and the assumption of fixed natural mortality likely results in assessment errors. However, estimation of temporal variation in natural mortality in stock assessments is rare (Brodziak et al., 2011). While this is a topic of ongoing research and progress is being made (e.g., Hollowed et al., 2000; Lee et al., 2011; Deroba and Schueller, 2013), challenges remain (e.g., Maunder and Wong, 2011; Francis, 2012) and incorporation of time-varying mortality into stock assessments has been slow and largely limited to a few taxa (Deroba and Schueller, 2013).

Cohort reconstructions or virtual population analyses (Hilborn and Walters, 1992) performed on tagged cohorts of salmon are the backbone of salmon stock assessment (e.g., Mohr, 2006; O'Farrell et al., 2012; PSC CTC, 2014). Reconstruction of cohorts from coded wire tag recovery data (Nandor et al., 2010) allows estimation of age-specific abundance, harvest rates, maturation rates, and other vital rates used for salmon management. An assumption of known, and typically invariant, natural mortality rates for adult salmon is required for statistical identifiability when using current techniques that treat cohorts independently (Hankin et al., 2005). Unfortunately, this means that vital rate estimates are biased to an unknown extent by assumed and arbitrary values assigned to adult natural mortality rates. For example, a real increase in the natural mortality rate between age 2 and age 3 in a particular year could be erroneously interpreted instead as unusually high maturation at age 2 and low early life survival for the corresponding cohort.

Biased vital rates are an obvious problem for management models. In addition, such biases may impair ecological or evolutionary insights when cohort reconstruction results are used, for example, to explore putative drivers of variation in maturation rates (e.g., Hankin and Logan, 2010) or juvenile survival (Sharma et al., 2013; Kilduff et al., 2014). In addition, it is of course impossible to explore the role of environmental conditions or predators (Hilborn et al., 2012) in driving variation in adult natural mortality if such mortality is *a priori* assumed to be constant.

This paper therefore has two major goals. First, we use simulation studies to thoroughly explore the sensitivity of results from traditional cohort reconstructions assuming known, temporally invariant adult natural mortality to misspecification of mean mortality rates and to variability in mortality rates. Second, we explore the potential for direct estimation of time-varying adult natural mortality rates for a range of biological scenarios. The existing literature on salmon population dynamics uses the terms “rate”, “fraction”, “probability”, and “proportion” in ways that are not always consistent. Unless we make specific reference to instantaneous rates when referring to other studies, the word “rate” is used throughout this paper, along with a unitless number, to represent the conditional probability or proportion of fish making a specified transition over one time step of the model. This is consistent with use of the term “rate” in cohort reconstruction models used by the Pacific Salmon Commission (e.g., PSC CTC 2014) and Pacific Fishery Management Council (e.g., O’Farrell et al. 2012).

3 Methods

Virtual population analysis (or cohort analysis) is applied to catch-at-age data to back calculate the number of individuals alive prior to a mortality event, with the goal of obtaining abundance estimates and mortality rates (e.g., Fry, 1949; Pope, 1972). This method requires a known terminal fishing mortality rate for the maximum age and specified natural mortality rates. Classical analyses of this type are deterministic in that the stochastic variation inherent in the data is not accounted for, and the accompanying model is fully saturated (no degrees of freedom); thus measures of statistical uncertainty are not readily available (Megrey, 1989).

A model resembling the classical virtual population analysis of Pope (1972) is applied to the management of Pacific Salmon stocks (e.g., Mohr, 2006; O'Farrell et al., 2012; PSC CTC, 2014). This model, termed cohort reconstruction, employs a monthly rather than annual time step, but similar to Pope (1972), a pulse fishery occurs at the start of each time step followed by natural mortality (Xiao and Wang, 2007). For the cohort reconstruction, the final time step in each year includes an additional mortality event, maturation, and a terminal maturation rate of 1.0 is required as opposed to a specified terminal fishing mortality rate. Additionally, cohort reconstruction methods estimate monthly or annual, rather than instantaneous, mortality rates and include an accounting for incidental fishing mortality.

Since the monthly models simply apportion a constant annual natural mortality rate across months, and depend on detailed month-specific harvest data and assumed mortality of discards, we chose an annual model for tractability, interpretability, and faster simulation. We did not explicitly model incidental fishing mortality, assuming it was incorporated into catch estimates. This cohort reconstruction (CR, abbreviations are defined in Table 1) assumes an annual sequence of discrete mortality events: ocean fishery mortality followed by maturation followed by ocean natural mortality. (Fish that mature return to the river where they are either caught in river fisheries or spawn and die shortly thereafter.) This reconstruction, in common with similar methods, requires a fixed age 2, 3, and 4 ("adult") natural mortality rate specified *a priori*. It is equivalent to Pope's (1972) cohort analysis when catch also includes escapement and fish are instantaneously removed from the population at the beginning of the year (Xiao and Wang, 2007).

We develop our example based on a subset of the data available on cohorts of hatchery-reared salmon tagged in distinct release groups using a coded wire tag (Nandor et al., 2010), specifically yearling releases of Klamath River fall Chinook salmon produced at Iron Gate Hatchery, California. We assume that a single cohort of age 1 coded wire tagged fish is released annually, that these fish are not subject to the ocean fishery or maturation at age 1, and that fish live a maximum of five years (all age 5 fish that survive the ocean fishery mature). Fish age increments by one year following the ocean natural mortality period. We index cohorts by i, $i = 1, 2, \ldots, I$, for I years of releases, with i equal to the birth year of a cohort (i.e., cohort i is released at age 1 in year $i + 1$). For cohort i, with R_i tagged fish released in October, fish first face juvenile mortality risk until April, then mortality from fishing, then removals for maturation in September, and then the cycle of potential mortality sources repeats annually for adults, with natural mortality now reflecting over-winter natural mortality in the ocean. This model structure implies a sequence of mortality outcomes at age a: the number caught in the ocean fishery, C_{ia}; the number that matured and returned to freshwater, M_{ia}; and the number that died from natural mortality, D_{ia} (symbols are defined in Table 2). However, $\{C_{ia}, M_{ia}, a = 2, 3, 4, 5\}$ are observable, whereas $\{D_{ia}, a = 1, 2, 3, 4\}$ are not; only the total natural mortality across ages is indirectly observable as $D_{i+} = \sum_{a=1}^{4} D_{ia} = R_i - \sum_{a=2}^{5}(C_{ia} + M_{ia})$. Although observable, the C_{ia} and M_{ia} quantities themselves are estimated, denoted by $\hat{C}_{ia}$ and $\hat{M}_{ia}$, by expanding the observed number of tag recoveries in a sampling stratum by the inverse of the sampling fraction and summing over the strata involved, respectively. $\hat{C}_{ia}$ can also include an accounting for incidental fishing mortality.

3.1 Cohort reconstruction

Given the estimates $\{\hat{C}_{ia}, \hat{M}_{ia}, a = 2, 3, 4, 5\}$ for cohort i, abundance is reconstructed from the oldest age to the youngest age by assuming that the adult natural mortality rates at age 2, 3, and 4 are known ($\tilde{d}_{i2} = \tilde{d}_{i3} = \tilde{d}_{i4} = 0.2$), and estimating the number alive at the beginning of age a as

$$\hat{N}_{ia} = \begin{cases} \hat{C}_{ia} + \hat{M}_{ia} + \dfrac{\hat{N}_{i\,a+1}}{1-\tilde{d}_{ia}}, & a = 2,3,4 \\ \hat{C}_{ia} + \hat{M}_{ia} & a = 5. \end{cases} \tag{1}$$

The $\{\hat{N}_{ia}\}$ estimates then permit estimation of the age-specific ocean exploitation (c_{ia}) and maturation (m_{ia}) rates for the cohort, along with the juvenile natural mortality rate (d_{i1}):

$$\hat{c}_{ia} = \frac{\hat{C}_{ia}}{\hat{N}_{ia}}, \quad \hat{m}_{ia} = \frac{\hat{M}_{ia}}{\hat{N}_{ia} - \hat{C}_{ia}}, \quad a = 2,3,4,5 \tag{2}$$

and

$$\hat{d}_{i1} = 1 - \frac{\hat{N}_{i2}}{R_i}, \tag{3}$$

respectively. Abundances and vital rates are estimated separately for each cohort, $i = 1, 2, \ldots, I$.

We explore the sensitivity of the above CR model estimates to assumptions about adult natural mortality using methods described in Section 3.3 and present the results in Section 4.1.

3.2 Separable cohort reconstruction

To estimate temporally varying natural mortality, we extend previous work by Hankin and Mohr (1993), which was based on band recovery models (e.g., Seber, 1970; Brownie et al., 1985) and a separable model decomposing vital rates into year and age effects (Pope, 1974; Doubleday, 1976; Kope, 1987). This approach is broadly applicable to any population where the recovery of individuals that share vital rates is tracked across a progression of possible fates and this progression can be reasonably approximated as a series of conditionally independent binomial processes. Through the sharing of certain year and age effects across cohorts, or cohort and age effects across years, it is possible with this stochastic, separable cohort reconstruction (SCR) model to estimate adult natural mortality rates in addition to the exploitation, maturation, and juvenile natural mortality rates by reducing the number of parameters to be estimated. Note that the CR model is normally applied to a single cohort, or as in this case, applied independently to multiple cohorts. The SCR models, in contrast, link cohorts across years and cannot be applied independently to a single cohort.

3.2.1 Stochastic basis

We begin by recasting the CR model for cohort i as a sequence of conditionally independent binomial events that results in the $\{C_{ia}\}, \{M_{ia}\}, \{D_{ia}\}$ outcomes given the number alive at the beginning of the respective period:

$$(4) \qquad \begin{aligned} C_{ia} &\sim \text{binomial}(N_{ia}, c_{ia}), && a = 2,3,4,5 \\ M_{ia} &\sim \text{binomial}(N_{ia} - C_{ia}, m_{ia}), && a = 2,3,4,5 \\ D_{ia} &\sim \text{binomial}(N_{ia} - C_{ia} - M_{ia}, d_{ia}), && a = 1,2,3,4 \end{aligned}$$

with $N_{i1} = R_i$, $C_{i1} = M_{i1} = 0$, $N_{i\,a+1} = N_{ia} - C_{ia} - M_{ia} - D_{ia}$, and $m_{i5} = 1$. This is equivalent to a multinomial distribution for the overall set of cohort i outcomes given the number initially released (Zippin, 1956):

$$(5) \qquad (\{C_{ia}\}, \{M_{ia}\}, \{D_{ia}\}) \sim \text{multinomial}(R_i; \{\pi_{C_{ia}}\}, \{\pi_{M_{ia}}\}, \{\pi_{D_{ia}}\}), \quad i = 1,2,\ldots,I$$

with the unconditional rates being defined as

$$(6) \qquad \pi_{C_{ia}} = S_{i\,a-1} c_{ia}, \quad \pi_{M_{ia}} = S_{i\,a-1}\,(1 - c_{ia})\,m_{ia}, \quad \pi_{D_{ia}} = S_{i\,a-1}\,(1 - c_{ia})\,(1 - m_{ia})\,d_{ia},$$

where S_{ia} is the probability that a cohort i fish survives all events from the time of release at age 1 through the end of age a:

$$S_{ia} = \begin{cases} 1 - d_{ia}, & a = 1 \\ S_{i\,a-1}\left(1 - c_{ia}\right)\left(1 - m_{ia}\right)\left(1 - d_{ia}\right), & a = 2, 3, 4. \end{cases} \tag{7}$$

This result leads directly to the distribution for the observable cohort i data:

$$(\{C_{ia}\}, \{M_{ia}\}, D_{i+}) \sim \text{multinomial}(R_i; \{\pi_{C_{ia}}\}, \{\pi_{M_{ia}}\}, \pi_{D_{i+}}), \quad i = 1, 2, \ldots, I \tag{8}$$

where $\pi_{D_{i+}} = \sum_{a=1}^{4} \pi_{D_{ia}} = 1 - \sum_{a=2}^{5}(\pi_{C_{ia}} + \pi_{M_{ia}})$. However, because R_i is large (typically $R_i > 10^5$) and $\pi_{D_{i+}}$ is close to one (typically $\pi_{D_{i+}} > 0.95$) this distribution can be approximated as a product of independent Poisson distributions having an equivalent set of expectations (McDonald, 1980):

$$(\{C_{ia}\}, \{M_{ia}\}) \sim \prod_{a=2}^{5} \text{Poisson}(R_i\, \pi_{C_{ia}}) \cdot \text{Poisson}(R_i\, \pi_{M_{ia}}), \quad i = 1, 2, \ldots, I, \tag{9}$$

with $D_{i+} = R_i - \sum_{a=2}^{5}(C_{ia} + M_{ia})$. Finally, assuming statistically independent outcomes among cohorts, the overall catch and maturation dataset is distributed approximately as

$$(\{C_{ia}\}, \{M_{ia}\}) \sim \prod_{i=1}^{I} \prod_{a=2}^{5} \text{Poisson}(R_i\, \pi_{C_{ia}}) \cdot \text{Poisson}(R_i\, \pi_{M_{ia}}), \tag{10}$$

with the $\{\pi_{C_{ia}}\}$ and $\{\pi_{M_{ia}}\}$ being functions of the $\{c_{ia}\}$, $\{m_{ia}\}$, and $\{d_{ia}\}$ vital rates (equations (6) and (7)).

3.2.2 Model identifiability

For some models, speaking generally, it is not possible to estimate all of the parameters due to the structure of the model, and such models are said to be non-identifiable. Non-identifiability can occur if a model is over-parameterized, where the model contains more parameters than there are observed variables. In addition, non-identifiability can occur due to parameter redundancy, where two or more parameters are confounded (they appear only as a product), in which case the model could be rewritten in terms of a smaller number of compounded parameters (see e.g. Cole et al., 2010, their example 1).

Various methods exist for detecting non-identifiability if it is not obvious. A numeric method exists that involves examining the rank of the Hessian matrix (Viallefont et al., 1998), and it is easily implemented since software packages often find the Hessian matrix numerically as part of the process of estimating the standard errors of parameters. However, this method can lead to incorrect conclusions, as demonstrated by Cole and Morgan (2010). To accurately determine whether or not a model is identifiable, symbolic algebra can be used (Cole et al., 2010) but this is complicated for complex models such as the SCR models evaluated in this paper. Instead we use a hybrid symbolic-numerical method (Choquet and Cole, 2012) to determine identifiability of the SCR models presented in this paper. It is both accurate and relatively straightforward to use.

Even in the absence of over-parameterization or parameter redundancy, non-identifiability can be caused by datasets with zero values (Cole et al., 2012). For all of the SCR models described in Section 3.2.3 below, we found that as long as the dataset contains no zero values, all parameters are identifiable.

3.2.3 Separable model variants

The CR model assumes that the vital rates $\{c_{ia}\}$, $\{m_{ia}\}$, and $\{d_{ia}\}$ are all cohort-age-specific (or year-age-specific), and thus is over-parameterized given that the $\{D_{ia}\}$ are unobservable. The CR estimation approach of treating the $\{d_{ia}\}$ as known is one way of reducing the number of parameters to be estimated from the dataset. Alternatively, one might assume that certain vital rates are shared among cohorts, years, or ages, or that the vital rates are a function of a reduced number of separable effects regarding cohort, year or age. With this additional imposed structure, it is possible to directly estimate the natural mortality rate.

The separable model form that we adopt presumes that the effects of cohort and age, or year and age on a vital rate are additive on the complementary log-log scale (McCullagh and Nelder, 1989). That is, for a particular vital rate p we assume that

$$g(p) = \log(-\log(1-p)) \tag{11}$$

is an additive function of these effects. The complementary log-log scale was adopted for two reasons. First, its use guarantees that the estimated vital rates will satisfy $0 < \hat{p} < 1$. Second, an additive model on this scale corresponds to the standard fishery mortality model for a Type 1 fishery (Ricker, 1975): $u_{ya} = 1 - \exp(-q_a f_y)$, where u_{ya} is the exploitation rate in year y of age a, f_y is the fishing effort in year y, and q_a is the catchability of age a. Thus, $g(u_{ya}) = \log(f_y) + \log(q_a)$ is an additive function of year and age effects.

We evaluated four SCR model variants (SCR-1, SCR-2, SCR-3, SCR-4) that imposed this additional structure on the $\{c_{ia}\}$, $\{m_{ia}\}$, and $\{d_{ia}\}$ rates. All four variants assumed that certain vital rates are shared among ages in a given year, or among years at a given age, and were based on our experience with Chinook salmon life history and fisheries, and the results of previous CR analyses of Chinook salmon. Specifically, we assume that: (1) age 4 and age 5 fish are fully vulnerable to the fishery, and experience the same exploitation rate in any given year; (2) the age 4 maturation rate is time invariant; and (3) the natural mortality rate in any given year is equal among adults (ages 2, 3, 4) but differs from that of the juveniles (age 1), letting a' denote the juvenile (J) and adult (A) age-classes:

$$a' = \begin{cases} J, & a = 1 \\ A, & a = 2, 3, 4. \end{cases} \tag{12}$$

All four SCR model variants also include separable age and year effects on $\{c_{ia}\}$, but differ depending on whether separable age and year or cohort effects were imposed on the $\{m_{ia}\}$

and/or $\{d_{ia}\}$.

SCR-1

This model assumes that the maturation rate for age 2 and age 3 fish is a non-separable function of age and cohort (the effect of age depends on the cohort), and that the natural mortality rate for juveniles and adults is a non-separable function of age-class and year (the effect of age-class depends on the year):

(13) $$g\left(c_{ia}\right) = \eta_y + \lambda_a, \quad y = i + a$$

(14) $$g\left(m_{ia}\right) = \begin{cases} \phi_{ia}, & a = 2, 3 \\ \psi, & a = 4 \end{cases}$$

(15) $$g\left(d_{ia}\right) = \tau_{ya'}, \quad y = i + a,$$

with $\lambda_4 = \lambda_5 = 0$ so that η_y reflects the fully vulnerable fishing mortality rate in year y.

For the first cohort, the d_{11}, c_{12}, m_{12}, and d_{12} rates depend on four effects parameters (τ_{2J}, η_3, ϕ_{12}, τ_{3A}) that are unique to those rates and are thus not identifiable given the dataset configuration. To make the SCR-1 model identifiable, for the first cohort we instead directly estimate the unconditional rates $\pi_{C_{12}}$, $\pi_{M_{12}}$, and S_{12}, on the complementary log-log scale, as single parameters rather than factoring them into their constituent vital rates with associated cohort and age, or year and age effects. Thus, the overall set of SCR-1 parameters to be estimated is

(16) $$\boldsymbol{\theta}_1 = \{\{\eta_y\}, \{\lambda_a\}, \{\phi_{ia}\}, \psi, \{\tau_{ya'}\}, g\left(\pi_{C_{12}}\right), g\left(\pi_{M_{12}}\right), g\left(S_{12}\right)\}.$$

SCR-2

This model is like SCR-1, but the maturation rate for age 2 and age 3 fish is a separable function of cohort and age effects:

$$g\left(m_{ia}\right)=\begin{cases}\zeta_i+\delta_a, & a=2,3\\ \psi, & a=4,\end{cases} \tag{17}$$

with ζ_i defined as the cohort i effect relative to cohort 1 ($\zeta_1 = 0$), so that δ_a reflects the age a ($a = 2, 3$) maturation rate for cohort 1. The SCR-2 model is identifiable as defined, so that the overall set of parameters to be estimated is

$$\boldsymbol{\theta}_2 = \{\{\eta_y\}, \{\lambda_a\}, \{\zeta_i\}, \{\delta_a\}, \psi, \{\tau_{ya'}\}\}. \tag{18}$$

SCR-3

This model is like SCR-1, but the natural mortality rate for juvenile and adult fish is a separable function of year and age effects:

$$g\left(d_{ia}\right) = \xi_y + \gamma_{a'} \quad y = i + a, \tag{19}$$

with ξ_y defined as the year y effect relative to year 2 ($\xi_2 = 0$), so that $\gamma_{a'}$ reflects the age-class a' ($a' = J, A$) natural mortality rate for year 2. The SCR-3 model is identifiable as defined, so that the overall set of parameters to be estimated is

$$\boldsymbol{\theta}_3 = \{\{\eta_y\}, \{\lambda_a\}, \{\phi_{ia}\}, \psi, \{\xi_y\}, \{\gamma_{a'}\}\}. \tag{20}$$

SCR-4

This model assumes that the fishing mortality rate, maturation rate, and natural mortality rate are all separable functions of year and age, or cohort and age effects:

$$g\left(c_{ia}\right) = \eta_y + \lambda_a, \quad y = i + a \tag{21}$$

$$g\left(m_{ia}\right) = \begin{cases} \zeta_i + \delta_a, & a = 2, 3 \\ \psi, & a = 4, \end{cases} \tag{22}$$

$$g\left(d_{ia}\right) = \xi_y + \gamma_{a'}, \quad y = i + a, \tag{23}$$

with the parameter baseline effects defined as for models SCR-1, SCR-2, and SCR-3. The SCR-4 model is identifiable as defined, so that the overall set of parameters to be estimated is

$$\boldsymbol{\theta}_4 = \{\{\eta_y\}, \{\lambda_a\}, \{\zeta_i\}, \{\delta_a\}, \psi, \{\xi_y\}, \{\gamma_{a'}\}\}. \tag{24}$$

3.2.4 Maximum likelihood estimation

Maximum likelihood was used to estimate the SCR model parameters, $\boldsymbol{\theta}$, from which the $\{c_{ia}\}$, $\{m_{ia}\}$, and $\{d_{ia}\}$ rates were estimated by substitution of $\hat{\boldsymbol{\theta}}$ into equations (13)–(15), (17), (19), and (21)–(23), and applying the inverse of g. We took the likelihood to be the distribution specified by equation (10) when viewed as a function of the parameters $\{\pi_{C_{ia}}\}$ and $\{\pi_{M_{ia}}\}$ given the estimates $\{\hat{C}_{ia}\}$, $\{\hat{M}_{ia}\}$. Therefore, the log-likelihood function, $\ell(\boldsymbol{\theta})$, ignoring the constants $\log(\hat{C}_{ia}!)$ and $\log(\hat{M}_{ia}!)$, was

$$\ell(\boldsymbol{\theta}) = \sum_i \sum_a \left\{\hat{C}_{ia} \log\left(R_i \pi_{C_{ia}}\right) - R_i \pi_{C_{ia}}\right\} + \left\{\hat{M}_{ia} \log\left(R_i \pi_{M_{ia}}\right) - R_i \pi_{M_{ia}}\right\}, \tag{25}$$

where $\pi_{C_{ia}} = \pi_{C_{ia}}(\boldsymbol{\theta})$ and $\pi_{M_{ia}} = \pi_{M_{ia}}(\boldsymbol{\theta})$. We did not explicitly account for the sampling error of $\hat{C}_{ia}$ and $\hat{M}_{ia}$ as estimates of C_{ia} and M_{ia} in $\ell(\boldsymbol{\theta})$. This could be done by weighting the two curly-bracketed components of $\ell(\boldsymbol{\theta})$ by the inverse of the overall sampling fractions associated with $\hat{C}_{ia}$ and $\hat{M}_{ia}$, respectively. However, we did account for this sampling error when evaluating the estimation performance of the models (Sections 3.3 and 3.3.2).

A small penalty was subtracted from $\ell(\boldsymbol{\theta})$ whenever any of the $\{\pi_{C_{ia}}\}$ or $\{\pi_{M_{ia}}\}$ were near zero ($< 10^{-10}$) to prevent numerical instability when taking the log of a very small $R\pi$ product. The penalty was equal to

$$0.01 \sum_i \sum_a I_{C_{ia}} \left(10^{-10} - \pi_{C_{ia}}\right)^2 + I_{M_{ia}} \left(10^{-10} - \pi_{M_{ia}}\right)^2, \tag{26}$$

where I_z was 1 if $\pi_z < 10^{-10}$ and 0 otherwise.

We maximized $\ell(\boldsymbol{\theta})$ by minimizing $-\ell(\boldsymbol{\theta})$ via automatic differentiation using AD Model Builder (ADMB, Fournier et al., 2012), which requires starting values for all parameters. If $-\ell(\boldsymbol{\theta})$ has many local minima and the starting values are far from the global minimum, the resulting $\hat{\boldsymbol{\theta}}$ may be far from that which corresponds to the global minimum. In this case, the model may be sensitive to the initial conditions, making it necessary to start the minimization from multiple points to increase the chance of finding the global minimum. For an individual dataset, we attempted to fit each of the SCR models 100 times, each time generating starting values at random from *a priori* defined distributions (Supplementary Appendix A). For some attempts, ADMB stopped the minimization procedure prematurely and returned an error message, in which case model estimates were not produced. In other instances, estimates were returned but an error message indicated the corresponding Hessian may not be positive-definite or the corresponding maximum gradient component exceeded our convergence criterion (0.0001). We discarded such estimates but documented their frequency (Supplementary Appendix A). We note that these occurrences were mostly rare and were largely prevented by several techniques used to improve convergence, such as user defined boundaries and estimation phases (Supplementary Appendix A).

We defined a solution as unique if any estimated rate differed by at least 0.001 on the proportion scale. Within the parameter space searched, we confirmed the existence of a single global solution (i.e., only one unique solution minimized $-\ell(\boldsymbol{\theta})$) and to illustrate the complexity of the solution space we also documented the number of runs converging on local minima (i.e., unique solutions corresponding to values of $-\ell(\boldsymbol{\theta})$ greater than the identified minimum).

3.3 Performance evaluation

Performance of the CR and SCR estimation models was evaluated by simulating datasets using alternative sets of specified vital rates ("generating rates"), and then estimating the vital rates from these simulated data using the estimation models. The adult natural mortality generating rates evaluated included various constant and time varying scenarios. In all cases a constant adult natural mortality rate of 0.2 was assumed in the CR estimation model. The bias and accuracy of the CR and SCR model vital rate estimates were then assessed and examined as a function of the adult natural mortality generating rate specifications.

3.3.1 Simulation framework

Demographic stochasticity was simulated in all datasets using the cohort sequential binomial mortality model (equation (4)): catch followed by maturation followed by natural mortality. To account for the additional variation introduced into the process through the use of $\{\hat{C}_{ia}\}$ and $\{\hat{M}_{ia}\}$ as estimates of the realized $\{C_{ia}\}$ and $\{M_{ia}\}$ (i.e., sampling error), the numbers of fish sampled from ocean fisheries and escapement areas were then simulated as additional binomial processes given the realized mortality model outcomes, assuming fixed sampling rates of 0.2 (Nandor et al., 2010) and 0.34 (Winship et al., 2013) respectively, and then expanded by the inverse of the respective sampling rate to simulate the $\{\hat{C}_{ia}\}$ and $\{\hat{M}_{ia}\}$ estimates used in the model estimation process. For each set of generating rates (described below), 100 independent datasets were simulated and fit to allow for assessment of the bias and accuracy (described in section 3.3.2) of the respective vital rate estimators.

Each set of generating rates consisted of values for the $\{c_{ia}\}$, $\{m_{ia}\}$, and $\{d_{i1}\}$ rates, along with the adult natural mortality rates. A detailed description of each set of generating rates follows, but we note first that in all cases the values for the $\{c_{ia}\}$, $\{m_{ia}\}$, and $\{d_{i1}\}$ rates were based on an actual set of estimates previously obtained for a series of 28 successive cohorts of Klamath River fall Chinook salmon yearlings released annually (one each year) from Iron Gate Hatchery (IGH) using the CR model assuming a constant adult natural mortality rate of 0.2. Because CR-derived estimates can be undefined when associated abundance estimates are zero, and can equal zero or one, we replaced in this set of estimates any undefined estimate with the corresponding mean rate, and any estimates equal to zero (one) with the next highest (lowest) estimated rate, and used linear interpolation to fill in rates for years with missing data. The resulting series of estimates ("IGH rates") are shown in Fig. 1. The simulated datasets were the same length as the IGH dataset (one cohort released each year for 28 successive years), and the number of yearling fish released for each cohort was 70,000 (the approximate average for the IGH dataset).

For evaluations involving the CR estimation model only, the time series of IGH rates were used as is for the generating rates in combination with both constant and variable adult natural mortality rates. Evaluated constant adult natural mortality rates, $\{d_{ia} = d_A, a = 2, 3, 4\}$, included $d_A = 0.02, 0.04, \ldots, 0.7$, resulting in 35 distinct sets of generating rates. To evaluate temporally variable (year-specific) adult natural mortality rates, $\{d_{ia} = d_{yA}, y = i + a, a = 2, 3, 4\}$, we considered two values for the mean rate, $\mu(d_{yA}) = 0.2, 0.4$, and coupled each with increasing coefficients of variation, $\mathrm{CV}(d_{yA}) = 0, 0.1, 0.2, \ldots, 0.5$. The d_{yA} generating rates were drawn at random from a beta distribution, $d_{yA} \sim \mathrm{Beta}(\alpha, \beta)$, with $\alpha = (1 - \mu)\mathrm{CV}^{-2} - \mu$ and $\beta = \alpha(\mu^{-1} - 1)$, where $\mu = \mu(d_{yA})$ and $\mathrm{CV} = \mathrm{CV}(d_{yA})$. For each of the twelve (μ, CV) combinations, 50 time series of year-specific adult natural mortality rates, $\{d_{yA}\}$, were drawn to improve the estimates of central tendency of the performance metrics described in Section 3.3.2. Together with the IGH rates, this resulted in a total of 600 (12×50) distinct sets of generating rates.

For evaluations involving both the CR and SCR models, four sets of generating rates were used. The first set of rates, "Con.2" (Constant, 0.2 annual adult natural mortality rate), were constant across years, with $d_A = 0.2$ and the remaining rates equal to the age-specific means of the IGH rates, as shown in Fig. 1. For the three remaining generating rate sets, the adult natural mortality rate varied across years. The second set of rates, "Var.2" (Variable, 0.2), used the time series of IGH rates as is along with a random sequence of temporally variable $\{d_{yA}\}$ with $\mu(d_{yA}) = 0.2$ and $\mathrm{CV}(d_{yA}) = 0.46$. The third set of rates, "Var.4" (Variable, 0.4), was identical to the second, except that $\mu(d_{yA}) = 0.4$ and $\mathrm{CV}(d_{yA}) = 0.38$. The final set of generating rates, "Add.2" (Additive, 0.2), adhered to the SCR-4 additive model structure (equations (21)–(23)), which satisfies the assumptions of all of the SCR model variants. A time varying sequence for each vital rate on the complementary log-log scale was obtained by adding a random year or cohort effect (as appropriate) drawn from a uniform(-0.9,0.9) distribution to $g(p)$, with p being the age-specific mean of the respective IGH rate (except for the age 4 maturation rate which was time invariant), with the same year effect added to juvenile and adult natural mortality. The resulting set of generating rates is shown in Fig. 1, with $\mu(d_{yA}) = 0.22$ and $\mathrm{CV}(d_{yA}) = 0.37$.

3.3.2 Performance metrics

To gauge the performance of the CR and SCR estimation models under the various simulation scenarios, we defined for each vital rate $p_{ia}, p = c, m, d$, the error in its estimated value for dataset k as $\hat{p}_{ia}(k) - p_{ia}(k)$, with $p_{ia}(k)$ being the actual, realized rate based on the binomial mortality model outcome for dataset k rather than the generating rate. For dataset k, we defined the mean error (ME) and root mean square error (RMSE) for age a over the $i = 1, 2, \ldots, I$ cohorts as

$$\mathrm{ME}(\hat{p}_a; k) = \sum_i \left[\hat{p}_{ia}(k) - p_{ia}(k)\right] \Big/ I, \tag{27}$$

$$\mathrm{RMSE}(\hat{p}_a; k) = \sqrt{\sum_i \left[\hat{p}_{ia}(k) - p_{ia}(k)\right]^2 \Big/ I}. \tag{28}$$

We then averaged each of these respective quantities over the replicate datasets to provide a measure of estimator bias ($\overline{\text{ME}}(\hat{p}_a)$) and accuracy ($\overline{\text{RMSE}}(\hat{p}_a)$), and regarded $|\overline{\text{ME}}(\hat{p}_a)| \leq 0.05$ and $\overline{\text{RMSE}}(\hat{p}_a) \leq 0.05$ as acceptable levels of performance. Note that because the ME and RMSE metrics involve averages taken over cohorts, they reflect (on average) the estimation errors expected in cohort-specific estimates.

For the CR model we also evaluated the performance of cohort abundance estimation. Because abundance at age differs greatly in terms of scale, we used the percent error in its estimated value for dataset k as the base metric, $\left[\hat{N}_{ia}(k) - N_{ia}(k)\right]/N_{ia}(k)$, with $N_{ia}(k)$ being the actual, realized abundance based on the binomial mortality model outcomes for dataset k rather than its expected value. For dataset k, we defined the mean percent error (MPE) and mean absolute percent error (MAPE) for age a over the $i = 1, 2, \ldots, I$ cohorts as

$$\text{MPE}(\hat{N}_a; k) = \sum_i \left(\left[\hat{N}_{ia}(k) - N_{ia}(k)\right]/N_{ia}(k)\right) \Big/ I, \tag{29}$$

$$\text{MAPE}(\hat{N}_a; k) = \sum_i \left|\left[\hat{N}_{ia}(k) - N_{ia}(k)\right]/N_{ia}(k)\right| \Big/ I. \tag{30}$$

We then averaged $\text{MPE}(\hat{N}_a; k)$ and $\text{MAPE}(\hat{N}_a; k)$ over the replicate datasets to provide a measure of estimator bias ($\overline{\text{MPE}}(\hat{N}_a)$) and accuracy ($\overline{\text{MAPE}}(\hat{N}_a)$), and regarded $|\overline{\text{MPE}}(\hat{N}_a)| \leq 0.2$ and $\overline{\text{MAPE}}(\hat{N}_a) \leq 0.2$ as acceptable levels of performance. Similarly, because the MPE and MAPE metrics involve averages taken over cohorts, they reflect (on average) the estimation errors expected in cohort-specific estimates.

Finally, for the CR model we also examined its ability to track temporal trends in the juvenile natural mortality rate, irrespective of whether the estimator itself is biased. For each dataset k we calculated Pearson's product-moment correlation coefficient between the estimated and the actual, realized set of juvenile natural mortality rates, $\rho(\hat{d}_1; k)$, averaged this over the replicate datasets to provide a measure of tracking ability ($\bar{\rho}(\hat{d}_1)$), and regarded $\bar{\rho}(\hat{d}_1) \geq 0.75$ as an acceptable level of performance.

Although all of these criteria for acceptable performance are somewhat arbitrary, we deemed them reasonable based on our experience participating in the management process for Pacific salmon fisheries. We note also that interpreting errors in values close to either 0.0 (i.e., maturation and exploitation rates for the youngest age classes) or 1.0 (i.e., juvenile natural mortality rate) can be problematic. For juvenile natural mortality, this problem can largely be alleviated by looking instead at percent error in reconstructed abundance at age, which is typically of more interest to managers due to its use in forecast models (e.g., Winship et al., 2015). Managers typically already regard estimates of maturation and exploitation rates for the youngest age classes with caution due to the small numbers of tag recoveries driving these estimates, and for exploitation rates there is additional uncertainty introduced by the large expansion factors and uncertain mortality rates needed to account for the discarding of sublegal-sized fish (e.g., Satterthwaite et al., 2013).

4 Results

4.1 CR model performance

With a constant adult natural mortality rate, estimated age 2 exploitation rates have acceptable bias and accuracy over the full range of d_A considered (owing in part to the small scale of these rates), and bias in exploitation rates for older ages remains acceptable in all cases considered except for age 3 if $d_A > 0.6$, while the accuracy is acceptable in all cases except for ages 3 and 4 if $d_A > 0.4$ (Fig. 2a). Variation in ME and RMSE over replicate datasets is greatest for age 3 and age 4, and this variation increases as d_A increases.

Although estimates of maturation rates at age 2 and age 4 are generally robust (Fig. 2b), age 3 rates are sensitive to misspecification of the adult natural mortality rate with $\overline{\mathrm{ME}}(\hat{m}_3) > 0.05$ for $d_A > 0.4$ and $\overline{\mathrm{ME}}(\hat{m}_3) > 0.15$ for $d_A > 0.6$. Acceptable levels of $\overline{\mathrm{RMSE}}(\hat{m}_3)$ occur for $d_A \leq 0.3$. Variation in ME over replicate datasets is minimal for all ages, whereas variation in RMSE is apparent for ages 3 and 4 and increases somewhat as d_A increases.

Juvenile natural mortality rates are estimated well by the CR model over the full range of d_A considered (Fig. 2c), although small errors in this rate can reflect large relative errors in (small) juvenile survival rates. Thus it is instructive to also consider errors in reconstructed abundance at age (Fig. 2d), especially for age 2 as this equals the estimated juvenile survival rate multiplied by the release group size. For age 2 abundance, the bias and accuracy are unacceptable unless $0.1 \leq d_A \leq 0.3$. Sensitivity of reconstructed abundance-at-age to misspecification of d_A is lower for older age classes, with both bias and accuracy acceptable for $d_A < 0.5$ for age 3 and over the full range of d_A considered for age 4. Little variation in the juvenile natural mortality rate and abundance-at-age bias and accuracy measures over replicate datasets was evident, except for age 4 with $d_A > 0.5$.

Vital rate estimation is less sensitive to variability in the adult natural mortality rate. When $\mu(d_{yA})$ matched the value assumed (0.2) in the CR model, all estimators meet the accuracy performance criteria over the full range of CV(d_{yA}) explored (Fig. 3, left column), and display little sensitivity to the amount of variability (all curves are nearly horizontal lines). Accuracy is lowest for the age 4 exploitation rate (due in part to the reduced abundance at age 4, and to the relatively low magnitude of the rate in contrast to the relatively high magnitude of the age 4 maturation rate).

When the adult natural mortality rate varies around a mean (0.4) which differs from the assumed value (Fig. 3, right column), sensitivity to variability increases (curvature is more apparent in the plots). Accuracy for age 3 exploitation rates is unacceptable for CV(d_{yA}) > 0.4, but for all other rates performance is either acceptable ($\hat{c}_2$, $\hat{m}_2$, $\hat{m}_4$, $\hat{d}_1$, $\hat{N}_3$, $\hat{N}_4$) or unacceptable ($\hat{c}_4$, $\hat{m}_3$, $\hat{N}_2$) over the full range of variability considered, with the $\hat{m}_3$ performance noticeably degrading as CV(d_{yA}) increases. Variation in the respective RMSE values over replicate datasets also increased, and in most cases increased further with increases in CV(d_{yA}).

Despite the difficulty in estimating age 2 abundance accurately when $\mu(d_{yA}) = 0.4$ (Fig. 3d, right column), estimates of the juvenile natural mortality rate did tend to track the simulated variation across years under several different combinations of $\mu(d_{yA})$ and CV(d_{yA}) values (Fig. 4). The mean correlation, $\bar{\rho}(\hat{d}_1)$, over the range of CV(d_{yA}) examined is very high when $\mu(d_{yA})$ is correctly specified (0.2), and remains above 0.9 even when $\mu(d_{yA})$ is 0.4 versus the specified 0.2, but falls below 0.75 when d_{yA} is both badly misspecified ($\mu(d_{yA}) =$ 0.6) and variable (CV(d_{yA}) > 0.35).

4.2 SCR model performance

The performance of the SCR-1 and SCR-2 models (jointly referred to below as SCR-1-2) was very similar overall, both in terms of bias (Fig. 5) and accuracy (Fig. 6). Likewise, the performance of the SCR-3 and SCR-4 models (jointly referred to below as SCR-3-4) was very similar overall (Figs. 5 and 6). And, in general, the SCR-3-4 models outperformed the SCR-1-2 models.

SCR-1-2 generally underestimated exploitation rates, maturation rates, and the juvenile natural mortality rate, and overestimated the adult natural mortality rate. The bias and accuracy of $\hat{m}_3$, $\hat{d}_J$, and $\hat{d}_A$, in particular, were unacceptable for most of the generating rate sets examined, and accuracy for the remaining estimated rates ($\hat{c}_3$, $\hat{c}_4$, $\hat{m}_4$) was unacceptable for Var.2 and Var.4. We therefore focus our attention below on the SCR-3-4 and CR model results.

For models SCR-3-4, unlike SCR-1-2, the adult natural mortality rate was not consistently positively biased across the generating rate sets but, as for SCR-1-2, when $\hat{d}_A$ was positively biased, the remaining estimated rates were negatively biased, and vice-versa. For Add.2 and Var.2, models SCR-3-4 were essentially unbiased for all rates (borderline for $\hat{d}_A$), and the accuracy was also mostly acceptable for Add.2 (nearly so for $\hat{d}_A$), but for Var.2 it was unacceptable for $\hat{c}_4$, $\hat{m}_3$, and $\hat{d}_A$. For Con.2 and Var.4, the $\hat{d}_A$ bias was unacceptable, and for Var.4 this was also the case for $\hat{m}_3$. For Con.2 and Var.4, the accuracy was unacceptable for $\hat{m}_3$ and $\hat{d}_A$, and for Var.4 this was also the case for $\hat{c}_3$ and $\hat{c}_4$. Variation in ME and RMSE over replicate datasets was greater for all rates with Con.2, and greatest for $\hat{m}_3$ and $\hat{d}_A$.

Considering the SCR-3-4 rates individually, the estimated exploitation rates had an acceptable bias, but the accuracy for $\hat{c}_3$ was unacceptable for Var.4, and for $\hat{c}_4$ the accuracy was unacceptable for Var.2 and Var.4. Estimated maturation rates had an acceptable bias except for $\hat{m}_3$ with Var.4, and an acceptable accuracy except for $\hat{m}_3$ with Con.2, Var.2, and Var.4. Variation in ME and RMSE over replicate datasets for $\hat{m}_3$ was relatively high for Con.2. The estimated juvenile mortality rate bias and accuracy was acceptable across all generating rate sets. For the estimated adult natural mortality rate, the bias was clearly unacceptable for Con.2 (biased high) and Var.4 (biased low), and the accuracy was unacceptable for all but the Add.2 generating rate set. And for $\hat{d}_A$, as for $\hat{m}_3$, variation in ME and RMSE over replicate datasets was relatively high for Con.2.

By comparison, the CR model was essentially unbiased (Fig. 5) for those generating rate sets in which d_A or $\mu(d_{yA})$ was equal to, or approximately equal to, the assumed constant value of 0.2 (Con.2, Add.2, Var.2), and its accuracy was also acceptable (Fig. 6), except in the case of $\hat{c}_4$ for Add.2. For the $\mu(d_{yA}) = 0.4$ generating rate set (Var.4), some bias was evident, most notably in the age 3 estimated rates. The pattern of this bias across the various rates was similar to that of the SCR-3-4 models for Var.4, with unacceptable performance (bias and accuracy) for $\hat{m}_3$, and borderline unacceptable accuracy for $\hat{c}_3$ and $\hat{c}_4$. Variation alone in d_A about the assumed constant value of 0.2 (Add.2 and Var.2 versus Con.2) had relatively little impact on estimator performance. The doubling of $\mu(d_{yA})$ to 0.4 versus the assumed constant value of 0.2 (Var.4 versus Con.2) resulted in acceptable performance except for $\hat{m}_3$ (accuracy of exploitation rates was borderline unacceptable).

Overall, the CR model performed as well as, or better than, the SCR-3-4 models. However, in the case of the Add.2 generating rate set, where the performance was mostly similar for the non-d_A estimated rates, the SCR-3-4 models were additionally able to estimate d_A reasonably well (the CR model assumes that d_A is known) and provided slightly better accuracy for some vital rates.

5 Discussion

5.1 CR model performance

Our evaluation of the performance of cohort reconstruction techniques across a wide range of plausible scenarios for salmon populations can serve to generally increase confidence in management applications of CR, and ecological inference using CR to estimate vital rates other than adult natural mortality, unless the adult natural mortality rate is at least twice as high as commonly assumed. Although the true adult natural mortality rate is unknown and surely varies (to an unknown extent), our results suggest only small consequences from assuming a known, constant adult natural mortality rate of 0.2 unless the true value exceeds approximately 0.4, or variability around an appropriately specified mean value substantially exceeds a CV of 0.5.

CR estimates of the age 2 abundance and age 3 maturation rate display the highest sensitivity to the misspecification of adult natural mortality rates, while juvenile natural mortality rates were well estimated over the entire range of adult natural mortality rates considered. However, it is important to realize that juvenile mortality rates are high and so juvenile survival, which is correspondingly small, may be estimated with more substantial relative error. Nevertheless, relative error in juvenile survival rates, like that of age 2 abundance, should be acceptably small (≤ 0.2) given adult natural mortality rates between 0.1 and 0.3. High correlation (≥ 0.75) between estimated and realized juvenile natural mortality rates suggest that, despite any bias introduced through misspecification of the mean adult natural mortality rate, and the difficulty of estimating the age 2 abundance accurately, temporal trends in the juvenile survival rate should be reliably detected unless adult natural mortality rates are very high (≥ 0.6) and highly variable (CV > 0.35).

The results of our performance evaluation of the CR model are mostly consistent with the conclusions reached by Hankin and Logan (2010) in an analysis of juvenile survival for salmon and for all vital rates in similar studies applied to long-lived iteroparous species.

Agger et al. (1973) and Ulltang (1977) found that when natural mortality is lower than assumed, fishing mortality is generally underestimated, and vice versa. For our analysis, this is most evident for the age 3 estimated exploitation rate. Agger et al. (1973) calculated that underspecification of the instantaneous natural mortality rate by 0.1 yr^{-1} results in a mean percent error of approximately 0.2 in the age 3 instantaneous fishing mortality rate, whereas we found an average percent error of 0.08 in this rate (after converting our exploitation and natural mortality rates to the instantaneous scale and assuming $d_A = 0.2$ versus an actual value of $d_A = 0.28$). Ulltang (1977) concluded that errors in fishing mortality and abundance estimates are likely to be small when the natural mortality rate fluctuates randomly around a correctly specified mean, similar to our results. We note however that our specific findings may not be broadly applicable outside the range of scenarios considered. For instance, Sims (1984) and Sampson (1988) found that the misspecification of natural mortality rates creates higher percent errors in estimates of abundance for lightly fished stocks. Indeed, when generating exploitation rates were halved in our analysis (not presented), the percent error of abundance estimates increased. Similarly, we would expect an increase (decrease) in accuracy with an increase (decrease) in the number of tagged fish released as juveniles.

Our estimation model performance metrics are defined relative to the realized demographic model outcomes and rates, and in this sense are conditional metrics. Thus, variation in the CR model estimates over replicate datasets, for example, was due primarily to sampling error (the use of sample-expanded estimates of catch and escapement) rather than demographic stochasticity. Alternative definitions for these performance metrics are of course possible. In particular, unconditional metrics could be defined relative to the demographic model expectations and generating rates. However, given that the focus of this paper is on the reconstruction of realized cohort outcomes and estimation of the associated rates, conditional performance metrics seem most appropriate. In addition, our simulated datasets were necessarily simplified compared to complications expected in real-world stock dynamics. For example, environmental conditions and their effects on vital rates are likely temporally autocorrelated, exploitation rates vary as a function of abundance forecasts which likely correlate with juvenile survival (e.g., Winship et al., 2015), and changes in fishery minimum size limits would be expected to change age effects on fishing mortality rates by changing the proportion of fish of legal size at each age. Increases in the number of tagged fish in each release group and/or sampling rates would be expected to reduce sensitivity to sampling and process error in the data and thereby improve the performance of CR models somewhat, but no increase in sample sizes can compensate for biases introduced by unmet assumptions. Implications of release group sizes and sampling rates for CR were discussed extensively by the PSC CWTWG (2008), so we did not explore sample sizes in further detail here.

5.2 SCR model performance

The ability to estimate time-varying natural mortality, maturation and exploitation rates simultaneously is expected to improve salmon assessments performed using cohort reconstruction methods. With increasing emphasis on determining relationships between environmental drivers and vital rates as well as synchrony in vital rates across release groups and populations (e.g., Sharma et al., 2013; Kilduff et al., 2014, 2015), there is also strong scientific motivation to ensure that the vital rates entering into these analyses are generated in the most rigorous way possible. Most applications of other salmon assessment models such as statistical catch-at-age models typically also require the assumption of known, constant adult natural mortality rates (e.g., Brenden et al., 2012), so the ability to quantify temporal variation in adult survival would have wide-ranging benefits.

That said, the SCR estimation models explored here all exhibited instances of unacceptable performance in at least some simulated scenarios, and would be ill suited for application to empirical datasets with no tag recoveries in particular age/stage categories. In addition, we have not (and could not have) rigorously tested all possible scenarios in which the model assumption of additive effects of year and age on vital rates might break down. Thus model results need to be interpreted with caution. Confidence in SCR model results when applied to an existing (real) dataset might be increased if multiple simulated datasets were generated based on the fitted vital rates, and the model did consistently well at estimating these generating vital rates across datasets.

Our results imply that the additive structure assumed for the maturation rates by models SCR-2 and SCR-4 did not lead to improved overall estimation performance versus SCR-1 and SCR-3, respectively. This may in part stem from the fact that the age 4 maturation rate was assumed to be constant for all SCR models. Thus although we considered an alternative SCR model formulation with constant maturation rates for each age, we expected this might do relatively little to improve model performance, and of course it would sacrifice the ability to estimate year-specific maturation rates. Our results also imply that the additive structure assumed for the natural mortality rates by model SCR-3 did lead to improved overall estimation performance versus SCR-1, regardless of whether the underlying rates were additive or not. In this case, since the juvenile mortality rates were well estimated under all scenarios (and thereby the year effects), the additive linkage presumably helped to resolve the overall adult age effect, scaling mean adult mortality relative to mean juvenile mortality but not necessarily tracking annual variation in adult natural mortality.

The performance of the SCR-3-4 estimation models when the adult natural mortality rate was a constant equal to 0.2 (Con.2), or was relatively high with a mean value of 0.4 (Var.4), was unacceptable for several rates. However, the performance was acceptable for all rates when the underlying natural mortality rates were variable with a mean of 0.2 and all vital rates were additive on the complementary log-log scale. Estimates were also essentially unbiased (in terms of the mean across cohorts/years) for all rates when the adult natural mortality rates were independently variable with a mean of 0.2 but the accuracy for several parameters, including the adult natural mortality rate, was unacceptable.

Overall, the alternative SCR models for estimating adult natural mortality rates directly did not clearly outperform the CR model in any of the scenarios we examined and proved sensitive to violations of functional assumptions and/or sampling variation. Although in some scenarios most parameter estimates from models SCR-3-4 were relatively robust to sampling variation, both models assume covariation between juvenile and adult natural mortality rates, and tracked juvenile natural mortality rates closely. Therefore even if they can unbiasedly estimate the mean adult natural mortality rate by fitting an appropriate age effect, the annual variation in adult natural mortality rate estimates will likely be driven by variation in juvenile natural mortality rates and thus may not provide real insight into true variation in adult natural mortality rates. As with the CR model, increases in the number of tagged fish in each release group and/or sampling rates would be expected to reduce sensitivity to sampling and process error in the data, but could not compensate for violation of model assumptions. Temporally autocorrelated environmental drivers likely lead to temporal autocorrelation in vital rates, with unknown implications for partitioning variation into year- versus age-effects. Future research could explore the implications of temporal autocorrelation, and the degree of correlation between juvenile and adult mortality, for the performance of the SCR approach described here. SCR model performance might be improved through approaches that incorporate autocorrelation into the estimation process (e.g., Johnson et al., 2016), or by developing a hierarchical approach to share information across release groups or stocks sharing a common ocean environment (e.g., Thorson et al., 2013).

5.3 Conclusions and recommendations

Taken together, our results suggest that CR methods are fairly robust in their applications to Pacific salmon unless common assumptions about adult natural mortality rates are seriously wrong. Because separable models SCR-3-4 were able to unbiasedly estimate the mean adult natural mortality rate under multiple sets of conditions conducive to CR, confidence in CR results might be increased if application of a model similar to SCR-3-4 yielded a mean adult natural mortality rate similar to that assumed in the CR, and that estimate might be used as the assumed natural mortality rate in a subsequent CR for the same or similar stocks. Given the apparent negative bias in adult natural mortality rate estimates from models SCR-3-4 when adult natural mortality rates are high and do not covary with juvenile natural mortality rates (Var.4), an acceptably low adult natural mortality rate estimate does not assure that CR results are reliable, but a high adult natural mortality rate estimate would be a definite cause for concern (although it should be noted that SCR-3-4 overestimated the adult natural mortality rate in the constant scenario, Con.2). Due to the limited accuracy of the SCR-3-4 models when the additivity assumptions are not met, these models may be less informative on whether adult natural mortality rates are unacceptably variable, unless there is strong reason to believe juvenile and adult natural mortality rates should covary.

In cases where SCR adult natural mortality rate estimates suggest application of typical CR may be problematic, managers and scientists would be wise to evaluate the sensitivity of key results and metrics to higher adult natural mortality rates and/or variable rates, as appropriate. It would also be advisable to consider all possible alternative sources of information on the adult natural mortality rate and the extent to which it might covary with the juvenile natural mortality rate (e.g., due to similarities or differences in feeding ecologies and spatial locations). Unless there is reason to believe the adult natural mortality rate has increased as a result of recent changes in the environment, one might also consider whether high estimates of adult natural mortality rates are consistent with expectations from life history theory if accompanied by low maturation rates (Mangel and Satterthwaite, 2008).

Direct estimation of adult natural mortality rates for salmon through other means has not received substantial attention in the published literature, but according to Hankin and Healey (1986), two empirical studies estimated an annual adult natural mortality rate of around 0.35 for Chinook salmon although maturation and mortality were confounded, suggesting actual mortality rates may have been lower. Thus, confidence in CR results could be improved in the future by field studies directly estimating adult natural mortality such as through adult tagging studies (Walters and Martell, 2004) which, if repeated over multiple years, could also yield insight into the degree of temporal variability in adult natural mortality and possibly insights into drivers of this variation. Such studies would be costly and logistically challenging, but the resulting insights could be highly worthwhile.

6 Acknowledgments

Model development was initiated under California Cooperative Fishery Research Unit Agreement No. 14-16-0009-1547, Research Work Order No. 32. Model refinement and simulation testing, along with manuscript preparation, were supported by NOAA Fisheries' Stock Assessment Analytical Methods (SAAM) program. We thank Steve Lindley, Michael O'Farrell, and two anonymous reviewers for helpful comments on earlier versions of this manuscript.

References

Agger, P., Boëtius, I., Lassen, H., 1973. Error in the Virtual Population Analysis: the effect of uncertainties in the natural mortality coefficient. J. Cons. Int. Explor. Mer 35 (1), 93.

Brenden, T.O., Bence, J.R., Szalai, E.B., 2012. An age-structured integrated assessment of Chinook salmon population dynamics in Lake Huron's main basin since 1968. Trans. Am. Fish. Soc. 141 (4), 919–933.

Brodziak, J., Ianelli, J., Lorenzen, K., Methot Jr, R.D., 2011. Estimating natural mortality in stock assessment applications. U.S. Department of Commerce, NOAA Technical Memorandum NMFS-F/SPO-119.

Brownie, C., Anderson, D.R., Burnham, K.P., Robson, D.S., 1985. Statistical inference from band recovery data: a handbook, second edition. U.S. Department of the Interior, Fish and Wildlife Service, Resource publication 156.

Choquet, R., Cole, D.J., 2012. A hybrid symbolic-numerical method for determining model structure. Math. Biosci. 236 (2), 117–125.

Cole, D.J., Morgan, B.J.T., 2010. A note on determining parameter redundancy in age-dependent tag return models for estimating fishing mortality, natural mortality and selectivity. J. Agric. Biol. Environ. Stat. 15 (4), 431–434.

Cole, D.J., Morgan, B.J.T., Catchpole, E.A., Hubbard, B.A., 2012. Parameter redundancy in mark-recovery models. Biom. J. 54 (4), 507–523.

Cole, D.J., Morgan, B.J.T., Titterington, D.M., 2010. Determining the parametric structure of models. Math. Biosci. 228 (1), 16–30.

Deroba, J.J., Schueller, A.M., 2013. Performance of stock assessments with misspecified age- and time-varying natural mortality. Fish. Res. 146, 27–40.

Doubleday, W.G., 1976. A least squares approach to analyzing catch-at-age data. ICNAF Res. Bull. 12, 69–81.

Fournier, D.A., Skaug, H.J., Ancheta, J., Ianelli, J., Magnusson, A., Maunder, M.N., Nielsen, A., Sibert, J., 2012. AD Model Builder: using automatic differentiation for statistical inference of highly parameterized complex nonlinear models. Optim. Method. Softw. 27 (2), 233–249.

Francis, R.I.C.C., 2012. The reliability of estimates of natural mortality from stock assessment models. Fish. Res. 119–120, 133–134.

Fry, F.E.J., 1949. Statistics of a lake trout fishery. Biometrics 5 (1), 27–67.

Goodyear, C.P., 1993. Spawning stock biomass per recruit in fisheries management: foundation and current use. In: Smith, S.J., Hunt, J.J., Rivard, D. (Eds.), Risk evaluation and biological reference points for fisheries management. No. 120. Canadian Special Publication of Fisheries and Aquatic Science, pp. 67–81.

Hankin, D.G., Healey, M.C., 1986. Dependence of exploitation rates for maximum yield and stock collapse on age and sex structure of chinook salmon (*Oncorhynchus tshawytscha*) stocks. Can. J. Fish. Aquat. Sci. 43 (9), 1746–1759.

Hankin, D.G., Logan, E., 2010. A preliminary analysis of Chinook salmon coded-wire tag recovery data from Iron Gate, Trinity River and Cole Rivers Hatcheries, brood years 1978–2004. Prepared for The Hoopa Valley Tribal Council and the Arcata Office, U.S. Fish and Wildlife Service. Available from https://www.fws.gov/arcata/fisheries/reports/technical/IGHTRH.CWTanalysis2009%20Hankin%20Rpt.pdf.

Hankin, D.G., Mohr, M.S., 1993. New methods for analysis of coded-wire tag recovery data: final report. Prepared for Trinity River Basin Field Office, U.S. Fish and Wildlife Service, Weaverville, California. Available from D.G. Hankin, Humboldt State University, Department of Fisheries Biology, Arcata, CA 95521.

Hankin, D.G., Morishima, G.S., Clark, J.H., Riddell, B.E., Deriso, R.B., Schwarz, C., Garza, J.C., Scott, J.B., 2005. Report of the expert panel on the future of the coded wire tag recovery program for Pacific salmon. Pacific Salmon Commission, Technical Report No. 18. Available from https://swfsc.noaa.gov/publications/FED/00791.pdf.

Hilborn, R., Cox, S.P., Gulland, F. M.D., Hankin, D.G., Hobbs, N.T., Schindler, D.E., Trites, A.W., 2012. The effects of salmon fisheries on southern resident killer whales: final report of the independent science panel. Prepared with the assistance of D.R. Marmorek and A.W. Hall, ESSA Technologies Ltd., Vancouver, B.C. for National Marine Fisheries Service (Seattle, WA) and Fisheries and Oceans Canada (Vancouver, BC). Available from http://www.westcoast.fisheries.noaa.gov/publications/protected_species/marine_mammals/killer_whales/esa_status/reflections1.pdf.

Hilborn, R., Walters, C.J., 1992. Quantitative fisheries stock assessment: choice, dynamics and uncertainty. Chapman and Hall, New York.

Hollowed, A.B., Ianelli, J.N., Livingston, P.A., 2000. Including predation mortality in stock assessments: a case study for Gulf of Alaska walleye pollock. ICES J. Mar. Sci. 57, 279–293.

Johnson, K.F., Councill, E., Thorson, J.T., Brooks, E., Methot, R.D., Punt, A.E., 2016. Can autocorrelated recruitment be estimated using integrated assessment models and how does it affect population forecasts? Fish. Res. 183, 222–232.

Kilduff, D.P., Botsford, L.W., Teo, S.L.H., 2014. Spatial and temporal covariability in early ocean survival of Chinook salmon (*Oncorhynchus tshawytscha*) along the west coast of North America. ICES J. Mar. Sci. 71 (7), 1671–1682.

Kilduff, D.P., Di Lorenzo, E., Botsford, L.W., Teo, S.L.H., 2015. Changing central Pacific El Niños reduce stability of North American salmon survival rates. Proc. Natl. Acad. Sci. U. S. A. 112 (35), 10962–10966.

Kope, R.G., 1987. Separable virtual population analysis of Pacific salmon with application to marked Chinook salmon, *Oncorhynchus tshawytscha*, from California's Central Valley. Can. J. Fish. Aquat. Sci. 44 (6), 1213–1220.

Lee, H.-H., Maunder, M.N., Piner, K.R., Methot, R.D., 2011. Estimating natural mortality within a fisheries stock assessment model: an evaluation using simulation analysis based on twelve stock assessments. Fish. Res. 109, 89–94.

Mangel, M., Satterthwaite, W.H., 2008. Combining proximate and ultimate approaches to understand life history variation in salmonids with application to fisheries, conservation, and aquaculture. Bull. Mar. Sci. 83 (1), 107–130.

Maunder, M.N., Wong, R.A., 2011. Approaches for estimating natural mortality: application to summer flounder (*Paralichthys dentatus*) in the U.S. mid-Atlantic. Fish. Res. 111, 92–99.

McCullagh, P., Nelder, J.A., 1989. Generalized linear models, second edition. Chapman and Hall, New York.

McDonald, D.R., 1980. On the Poisson approximation to the multinomial distribution. Can. J. Stat. 8 (1), 115–118.

Megrey, B.A., 1989. Review and comparison of age-structured stock assessment models from theoretical and applied points of view. In: Edwards, E.F., Megrey, B.A. (Eds.), Mathematical analysis of fish stock dynamics. Symposium 6. American Fisheries Society, pp. 8–48.

Mohr, M.S., 2006. The cohort reconstruction model for Klamath River fall Chinook salmon. Available from M.S. Mohr, National Marine Fisheries Service, 110 Shaffer Road, Santa Cruz, California 95060, USA.

Nandor, G.F., Longwill, J.R., Webb, D.L., 2010. Overview of the coded wire tag program in the greater Pacific region of North America. In: Wolf, K.S., O'Neal, J.S. (Eds.), PNAMP Special Publication: Tagging, telemetry and marking measures for monitoring fish populations—A compendium of new and recent science for use in informing technique and decision modalities. Pacific Northwest Aquatic Monitoring Partnership Special Publication 2010-002, pp. 5–46. Available from http://www.pnamp.org/sites/default/files/PNAMP_2010_002_TTMfirst.pdf

O'Farrell, M.R., Mohr, M.S., Grover, A.M., Satterthwaite, W.H., 2012. Sacramento River winter Chinook cohort reconstruction: analysis of ocean fishery impacts. U.S. Department of Commerce, NOAA Technical Memorandum NOAA-TM-NMFS-SWFSC-491.

Pope, J.G., 1972. An investigation of the accuracy of virtual population analysis using cohort analysis. ICNAF Res. Bull. 9, 65–74.

Pope, J.G., 1974. A possible alternative method to virtual population analysis for the calculation of fishing mortality from catch at age data. ICNAF Annual Meeting, June 1974, Research Document 74/20, Serial Number 3166. Available from http://icnaf.nafo.int/docs/1974/res-20.pdf.

PSC CTC (Pacific Salmon Commission Chinook Technical Committee), 2014. 2013 exploitation rate analysis and model calibration, volume 1. Pacific Salmon Commission, TCCHINOOK (14)-1 V.1. Available from http://www.psc.org/pubs/TCCHINOOK(14)-1_V1.pdf.

PSC CWTWG (Pacific Salmon Commission Coded Wire Tag Workgroup), 2008. An action plan in response to coded wire tag (CWT) expert panel recommendations. Pacific Salmon Commission, Technical Report No. 25. Available from http://www.psc.org/pubs/psctr25.pdf.

Ricker, W.E., 1975. Computation and interpretation of biological statistics of fish populations. Fisheries Research Board of Canada, Bulletin 191.

Sampson, D.B., 1988. The stability of Virtual Population Analysis cohort size estimates. J. Cons. Int. Explor. Mer 44 (2), 135–142.

Satterthwaite, W.H., Mohr, M.S., O'Farrell, M.R., Wells, B.K., 2013. A comparison of temporal patterns in the ocean spatial distribution of California's Central Valley Chinook salmon runs. Can. J. Fish. Aquat. Sci. 70, 574–584.

Seber, G.A.F., 1970. Estimating time-specific survival and reporting rates for adult birds from band returns. Biometrika 57 (2), 313–318.

Sharma, R., Vélez-Espino, L.A., Wertheimer, A.C., Mantua, N., Francis, R.C., 2013. Relating spatial and temporal scales of climate and ocean variability to survival of Pacific Northwest Chinook salmon (*Oncorhynchus tshawytscha*). Fish. Oceanogr. 22 (1), 14–31.

Sims, S.E., 1984. An analysis of the effect of errors in the natural mortality rate on stock-size estimates using Virtual Population Analysis (Cohort Analysis). J. Cons. Int. Explor. Mer 41 (2), 149–153.

Thorson, J.T., Stewart, I.J., Taylor, I.G., Punt, A.E., 2013. Using a recruitment-linked multispecies stock assessment model to estimate common trends in recruitment for US West Coast groundfishes. Mar. Ecol. Prog. Ser. 483, 245–256.

Ulltang, Ø., 1977. Sources of errors in and limitations of Virtual Population Analysis (Cohort Analysis). J. Cons. Int. Explor. Mer 37 (3), 249–260.

Viallefont, A., Lebreton, J.-D., Reboulet, A.-M., Gory, G., 1998. Parameter identifiability and model selection in capture-recapture models: a numerical approach. Biom. J. 40 (3), 313–325.

Walters, C.J., Martell, S.J.D., 2004. Fisheries ecology and management. Princeton University Press, New Jersey.

Winship, A.J., O'Farrell, M.R., Mohr, M.S., 2013. Management strategy evaluation applied to the conservation of an endangered population subject to incidental take. Biol. Cons. 158, 155–166.

Winship, A.J., O'Farrell, M.R., Satterthwaite, W.H., Wells, B.K., Mohr, M.S., 2015. Expected future performance of salmon abundance forecast models with varying complexity. Can. J. Fish. Aquat. Sci. 72, 557–569.

Xiao, Y., Wang, Y.-G., 2007. A revisit to Pope's cohort analysis. Fish. Res. 86 (2), 153–158.

Zippin, C., 1956. An evaluation of the removal method of estimating animal populations. Biometrics 12 (2), 163–189.

Table 1 Abbreviations used and their definition.

Abbreviation	Definition
IGH	Iron Gate Hatchery
ME	Mean error
RMSE	Root mean square error
MPE	Mean percent error
MAPE	Mean absolute percent error
CR	Cohort reconstruction
SCR	Separable cohort reconstruction
SCR-1	SCR model variant 1: Rates on complementary log-log scale: fishing mortality separable (age + year); maturation non-separable (age * cohort) for age 2 and 3, constant for age 4; natural mortality non-separable (age-class * year).
SCR-2	SCR model variant 2: Rates on complementary log-log scale: fishing mortality separable (age + year); maturation separable (age + cohort) for age 2 and 3, constant for age 4; natural mortality non-separable (age-class * year).
SCR-3	SCR model variant 3: Rates on complementary log-log scale: fishing mortality separable (age + year); maturation non-separable (age * cohort) for age 2 and 3, constant for age 4; natural mortality separable (age-class + year).
SCR-4	SCR model variant 4: Rates on complementary log-log scale: fishing mortality separable (age + year); maturation separable (age + cohort) for age 2 and 3, constant for age 4; natural mortality separable (age-class + year).
Con.2	Constant generating rates with an adult natural mortality rate of 0.2.
Var.2	Time varying generating rates with an adult natural mortality rate mean value of 0.2.
Var.4	Time varying generating rates with an adult natural mortality rate mean value of 0.4.
Add.2	Time varying generating rates with additive year and age or cohort and age effects on the complementary log-log scale and an adult natural mortality rate mean value of 0.22.

Table 2 Symbols used and their definition.

Symbol	Definition
$\hat{}$	Estimated quantity (overscript)
$\tilde{}$	Assumed quantity (overscript)
$\bar{}$	Average quantity (overscript)
i	Cohort (brood year), $i = 1, 2, \ldots, I$
a	Age, $a = 1, 2, \ldots, 5$
a'	Age class: J ($a = 1$) or A ($a = 2, 3, 4$)
y	Calendar year, $y = i + a$
k	Simulated dataset index, $k = 1, 2, \ldots$
R	Number of tagged fish released
N	Abundance
C	Ocean catch
M	River escapement
D	Natural mortality (deaths)
c	Exploitation rate
m	Maturation rate
d	Natural mortality rate
p	Conditional mortality rate (c, m, or d)
π	Unconditional mortality rate
S	Survival rate (from release)
$g()$	Complementary log-log function
$l()$	Log-likelihood function
$\boldsymbol{\theta}$	Parameter set (SCR models)
η	$g(c)$ year effect
λ	$g(c)$ age effect
ϕ	$g(m)$ cohort-age effect
ζ	$g(m)$ cohort effect
δ	$g(m)$ age effect ($a = 2, 3$)
ψ	$g(m)$ age effect ($a = 4$)
τ	$g(d)$ year-age-class effect
ξ	$g(d)$ year effect
γ	$g(d)$ age-class effect
μ	Mean value
ρ	Correlation coefficient
CV	Coefficient of variation

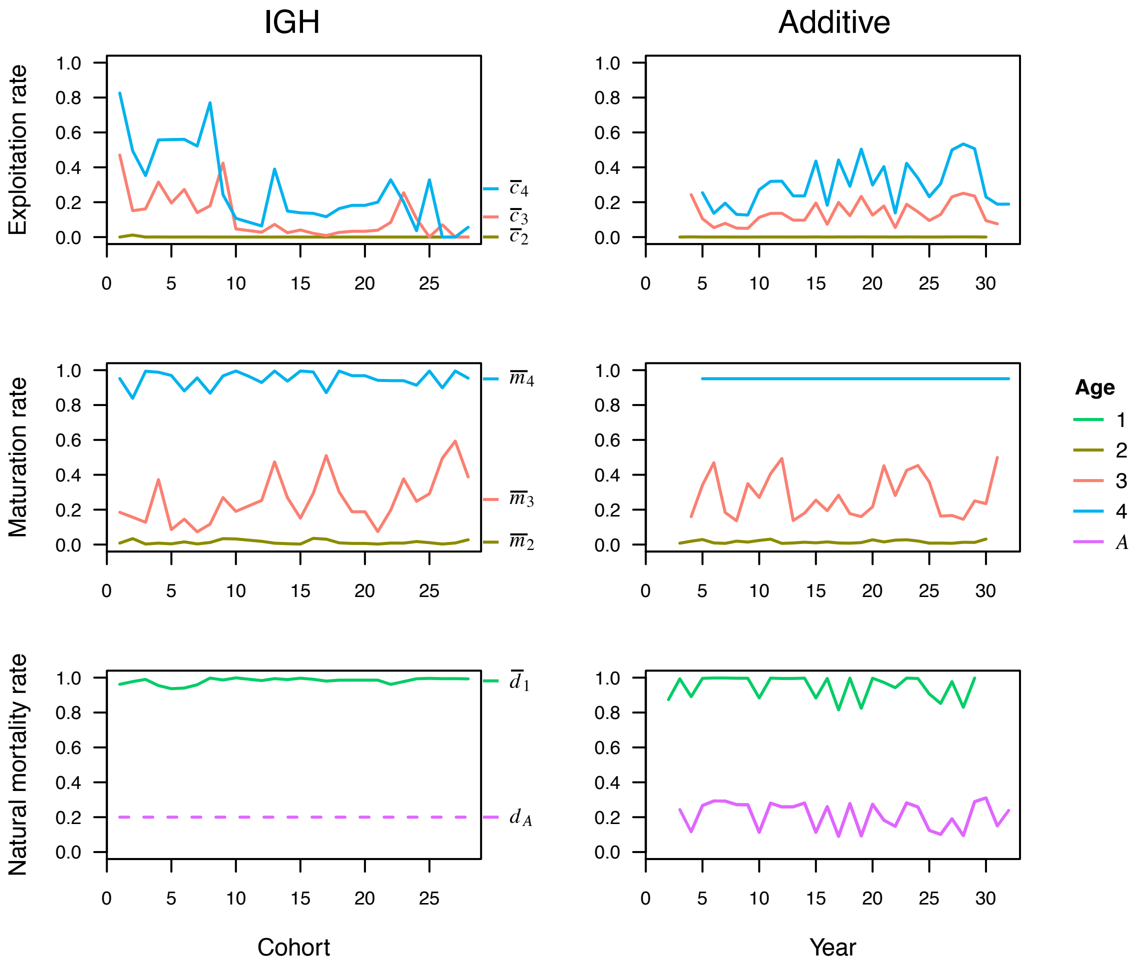

Fig. 1. Generating rates used for performance evaluation. Left column: IGH rates with mean values indicated on right vertical axis. Right column: additive (on complementary log-log scale) rates derived from IGH mean rates assuming SCR-4 model structure. Adult natural mortality is assumed fixed at 0.2 for the IGH rates (dashed line). The additive scenario is parameterized to yield mean and variability in vital rates comparable to IGH but with independently drawn random effects of years/cohorts.

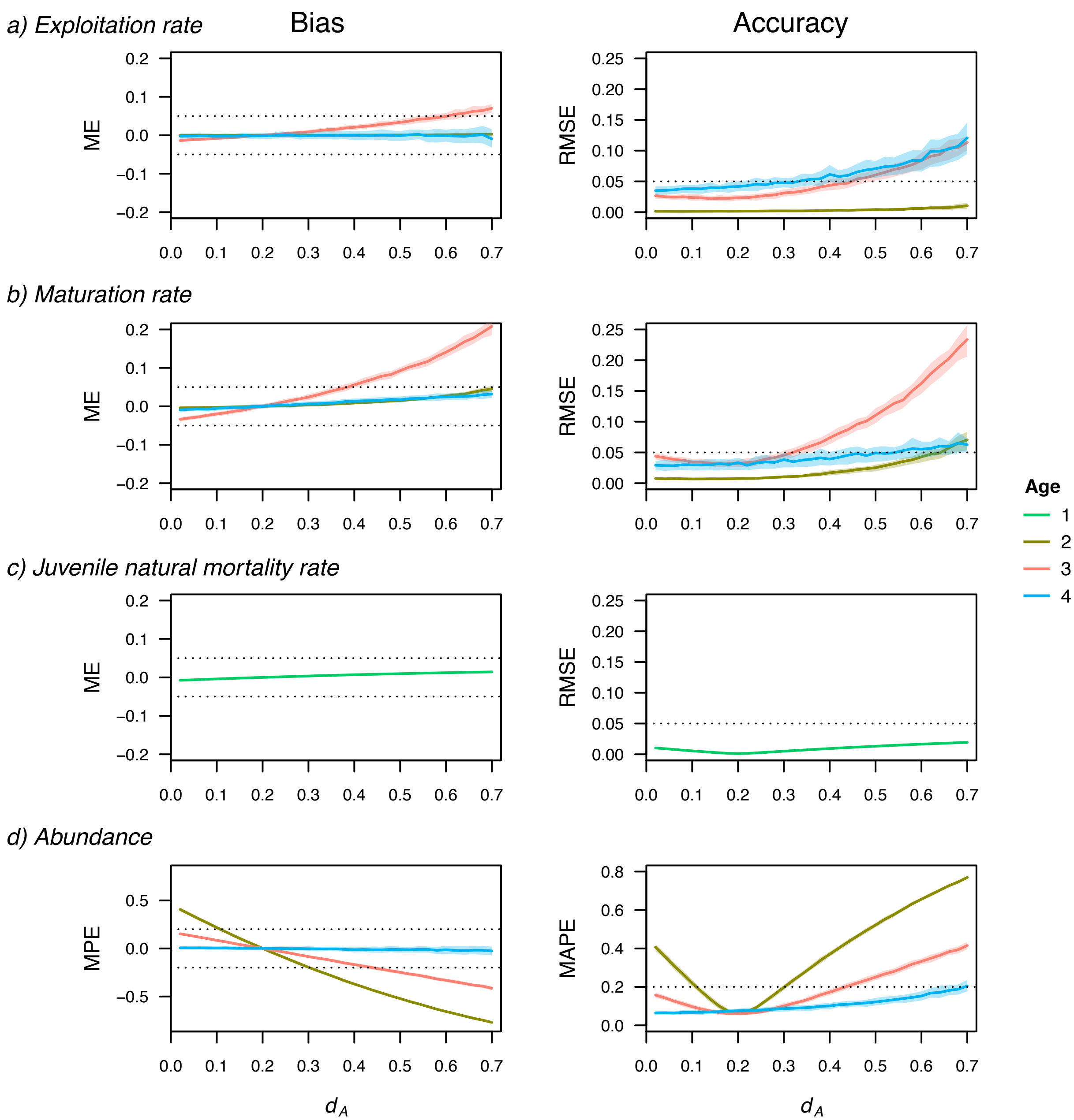

Fig. 2. CR estimation model performance when the underlying adult natural mortality rate is constant (d_A), but misspecified (assumed equal to 0.2). Solid lines indicate bias (left column) and accuracy (right column) as a function of the actual d_A value. Shaded regions about lines depict central 68% quantiles of respective metrics over replicate datasets. Dotted lines reference acceptable performance levels. Note scale of y-axis differs for abundance panels.

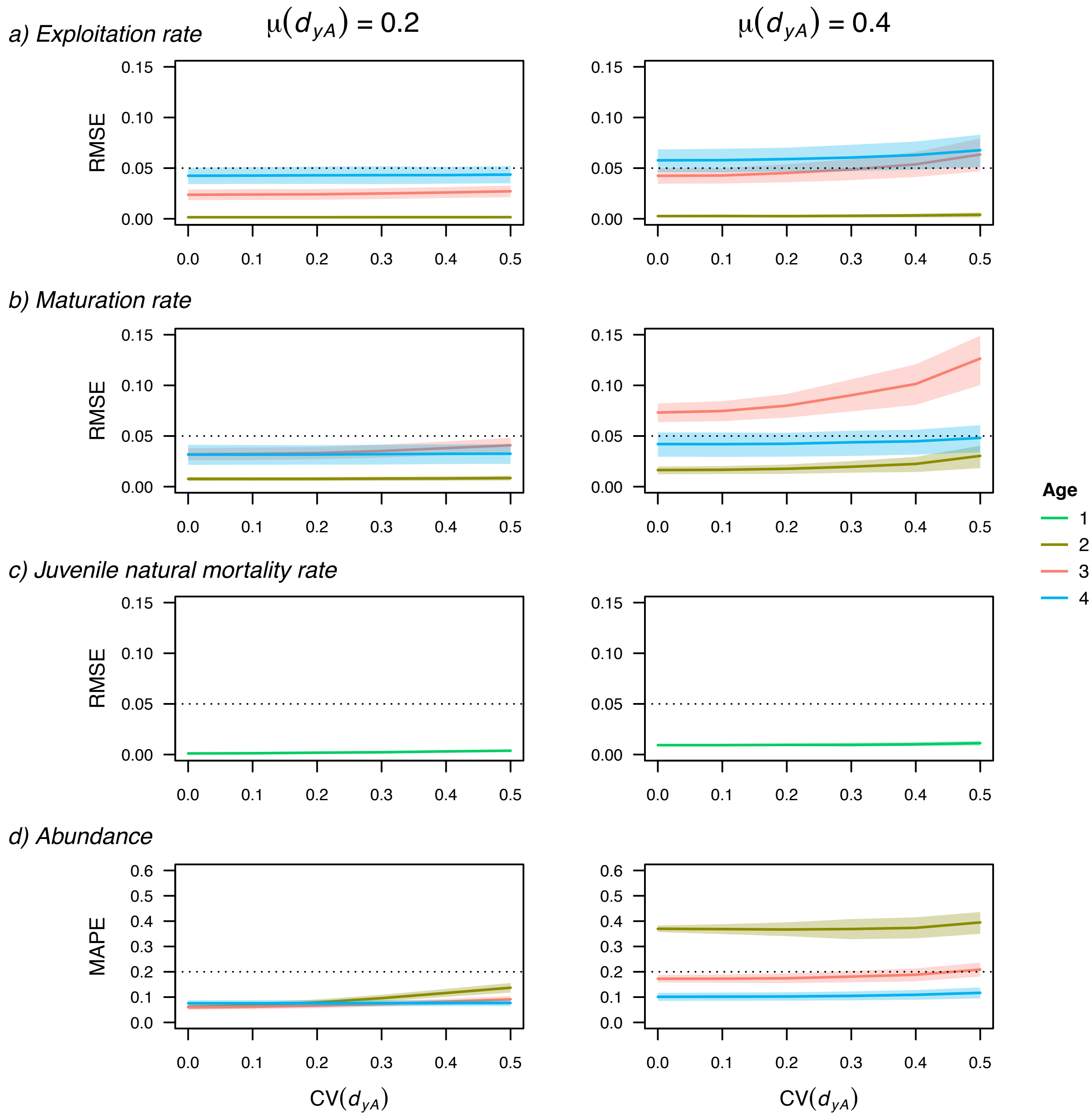

Fig. 3. CR estimation model accuracy measures when the underlying adult natural mortality rate is variable ($\{d_{yA}\}$), but assumed constant (equal to 0.2). Solid lines indicate accuracy as a function of the coefficient of variation when the mean rate is equal to the assumed constant (left column), and twice that of the assumed constant (right column). Shaded regions about lines depict central 68% quantiles of respective metrics over replicated datasets. Dotted lines reference acceptable performance levels. Note scale of y-axis differs for abundance panels.

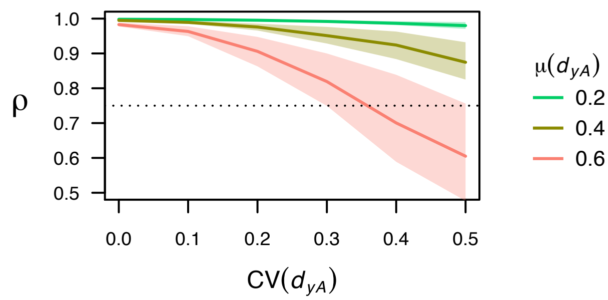

Fig. 4. CR estimation model ability to track temporal trends in the juvenile natural mortality rate when the underlying adult natural mortality rate is variable ($\{d_{yA}\}$), but assumed constant (equal to 0.2). Correlation (ρ) between the estimated and realized set of juvenile natural mortality rates as a function of the coefficient of variation when the mean rate is equal to, twice, or three times that of the assumed constant. Solid lines indicate mean correlation. Shaded regions about lines depict central 68% quantiles of ρ over replicated datasets. Dotted line references acceptable performance level.

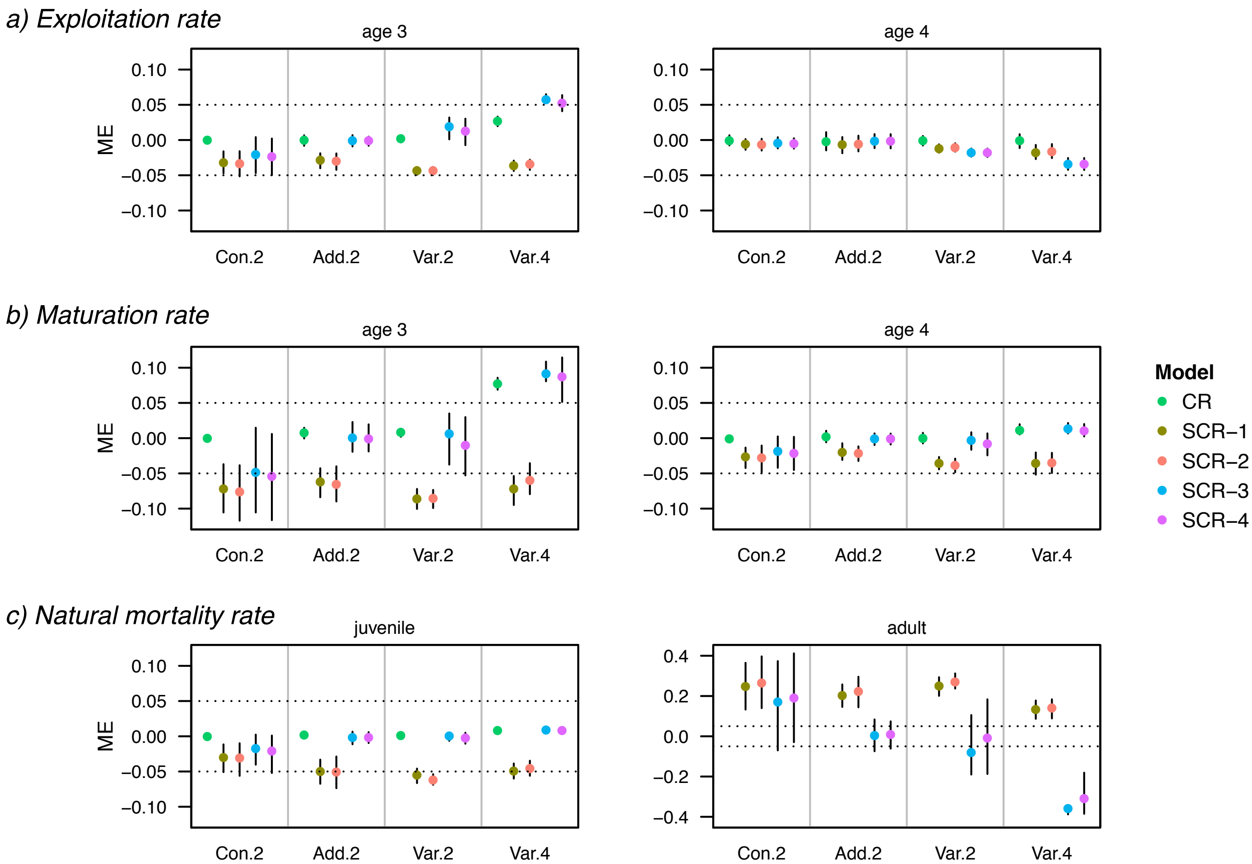

Fig. 5. SCR and CR estimation model bias for one constant (Con.2) and three variable (Add.2, Var.2, Var.4) generating rate scenarios (Figure 1): Con.2 rates are the IGH mean values with $d_A = 0.2$; Add.2 rates are additive on the complementary log-log scale with $\mu(d_{yA}) = 0.22$; Var.2 rates are the IGH rates with $\mu(d_{yA}) = 0.2$; Var.4 rates are the IGH rates with $\mu(d_{yA}) = 0.4$. In all cases, the CR model assumes the adult natural mortality rate is a constant equal to 0.2. Dots indicate bias, and vertical bars depict central 68% quantiles of the ME metric over replicate datasets. Dotted lines reference acceptable performance level. Note scale of y-axis differs for adult natural mortality rate panel.

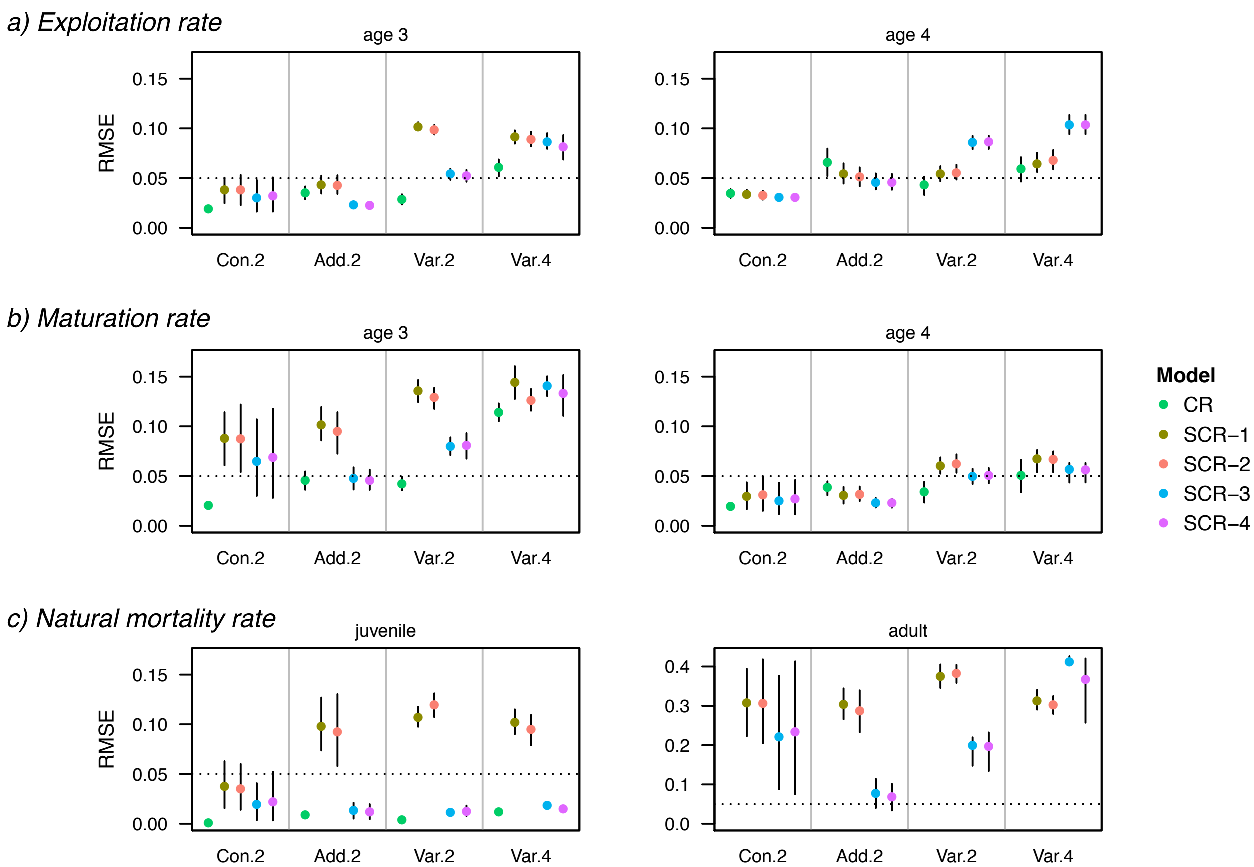

Fig. 6. SCR and CR estimation model accuracy for one constant (Con.2) and three variable (Add.2, Var.2, Var.4) generating rate scenarios (Figure 1): Con.2 rates are the IGH mean values with $d_A = 0.2$; Add.2 rates are additive on the complementary log-log scale with $\mu(d_{yA}) = 0.22$; Var.2 rates are the IGH rates with $\mu(d_{yA}) = 0.2$; Var.4 rates are the IGH rates with $\mu(d_{yA}) = 0.4$. In all cases, the CR model assumes the adult natural mortality rate is a constant equal to 0.2. Dots indicate accuracy, and vertical lines depict central 68% quantiles of the RMSE metric over replicate datasets. Dotted line references acceptable performance level. Note scale of y-axis differs for adult natural mortality rate panel.

Appendix A SCR model fitting and optimization

Starting values

ADMB, like many other nonlinear optimization routines, cannot exit from local minima, making it necessary to repeatedly fit the models starting from a wide range of initial values as opposed to only one set of values. We chose distributions of starting values with the goal of encompassing a wide, yet biologically plausible range. These ranges were either set to the parameter estimation boundary constraints (see below), or were narrowed slightly to increase the potential for convergence. Starting values for parameters on the complementary log-log scale were time invariant and drawn from normal distributions centered on the generating rates (averaged over years), but had relatively large variances. Randomly drawn values outside of the specified permissible range were truncated to the nearest range endpoint, and adjusted if necessary to satisfy any additional specified constraints among the parameters. Starting value distribution means and coefficients of variation, as well as the permissible ranges and additional specified constraints, are presented in Tables A.1, A.2, A.3, and A.4, for the SCR-1, SCR-2, SCR-3, and SCR-4 model variants, respectively. For reference, we also include in these tables the translation of these specifications to the vital rate (proportion) scale.

Boundaries and phase estimation

To increase the potential for convergence, we specified boundary constraints and the phase of estimation for each of the parameters to be estimated (Tables A.1, A.2, A.3, A.4). Boundary constraints ensured that the estimated parameters fell within a reasonable range and restricted the solution space. Phase estimation allowed us to specify when to initiate optimization for a given parameter within the overall search. This enabled difficult parameters to be estimated after other, less difficult to estimate parameters were at or near their optimal values. In each phase, the parameters activated in the current or previous phase were optimized using their estimated values in the previous phase as initial values.

Convergence performance

For each attempted fitting of an SCR model to a dataset using a randomly drawn set of starting values, we documented whether ADMB (a) failed to produce an estimate because the minimization procedure was terminated prematurely ("failed"), (b) produced an estimate but reported that the Hessian may not be positive-definite ("non-positive-definite Hessian"), (c) produced an estimate with a positive-definite Hessian, but the maximum gradient component exceeded our convergence criterion of 0.0001 ("convergence criterion not met"), or (d) produced an estimate with a positive-definite Hessian, and the maximum gradient component was less than or equal to our convergence criterion of 0.0001 ("convergence criterion met"). Over the 100 attempted fittings to the dataset, where the convergence criterion was met, we determined which estimate minimized the negative of the log-likelihood function (the maximum likelihood estimate), and also recorded the number of local minima (unique solutions in which at least one estimated vital rate differed by at least 0.001 from the maximum likelihood estimate). The frequency of the above outcomes for each of the SCR models and generating rate sets is shown in Table A.5, where the frequencies are over the 100 fitting attempts (averaged across the 100 independent datasets).

Overall, starting values leading to failure or non-positive-definite Hessian matrices occurred less than 1.6% of the time. And, other than for the SCR-4 model and Add.2 generating rate set, greater than 97.3% of the starting value sets led to the convergence criterion being met. For the Add.2 generating set, the convergence success rate was much lower: 43.9–77.7%. However, based on limited testing, we suspect that a slight increase in our convergence criterion (e.g., from 0.0001 to 0.001) would have resulted in a much higher convergence success rate for the Add.2 generating set, and few additional local minima. While the convergence rate for the SCR-4 model in particular was only 43.9% for this generating rate set, the SCR-4 convergence rate was 88.5–95.2% for the other generating rate sets. Note that in these cases of a lower convergence success rate, it was not primarily due to failure or a non-positive-definite Hessian, and multiple minima occurred less than 0.2% of the time. We also note that, anecdotally, in many instances in which the convergence criterion was not met, the estimate was in fact very close to the maximum likelihood estimate, but the minimization routine was terminated "early" relative to our criterion because it met one of the other ADMB built-in convergence criteria (Fournier, 2015). In general, the SCR models were not particularly difficult to fit once the user defined boundaries and estimation phases were appropriately set up, and we suspect that in an application consisting of a single, real dataset, the boundaries, phases, and convergence criterion could be fine-tuned to yield a high convergence success rate.

References

Fournier, D., 2015. AUTODIF: A C++ array language extension with automatic differentiation for use in nonlinear modeling and statistics, version 11.4. ADMB Foundation, Honolulu, available from http://admb-project.org/documentation/manuals.

Table A.1 Model SCR-1 parameter starting values and estimation specifications (upper portion), and translation of specifications to vital rate scale (lower portion).

	Starting Value				Estimation	
Parameter	Mean	CV	Range	Additional constraints	Bounds	Phase
η_y	$g(\bar{c}_4)$	0.4	$[-7.0, \ 0.5]$	$\eta_4 = \eta_5 = \ldots = \eta_{I+5} = \eta^*$	$[-7.0, \ 0.5]$	1
λ_2	$g(\bar{c}_2) - \eta^*$	0.4	$[-6.5, -2.2]$	$\lambda_2 \geq -9 - \eta^*$	$[-7.5, -2.0]$	1
λ_3	$g(\bar{c}_3) - \eta^*$	0.4	$[-6.5, -0.4]$	$\lambda_3 \geq -8 - \eta^*$, $\lambda_3 \geq \lambda_2$	$[-7.5, -0.1]$	2
ϕ_{i2}	$g(\bar{m}_2)$	0.4	$[-7.9, -1.2]$	$\phi_{22} = \phi_{32} = \ldots = \phi_{I2} = \phi_2^*$	$[-8.0, -1.0]$	3
ϕ_{i3}	$g(\bar{m}_3)$	0.4	$[-7.8, \ 1.9]$	$\phi_{13} = \phi_{23} = \ldots = \phi_{I3} = \phi_3^*$, $\phi_3^* \geq \phi_2^*$	$[-7.8, \ 2.0]$	3
ψ	$g(\bar{m}_4)$	0.4	$[\ 0.0, \ 1.9]$	$\psi \geq \phi_3^*$	$[\ 0.0, \ 2.0]$	1
τ_{yJ}	$g(\bar{d}_J)$	0.4	$[-0.3, \ 1.8]$	$\tau_{3J} = \tau_{4J} = \ldots = \tau_{I+1\ J} = \tau_J^*$	$[-0.4, \ 2.0]$	3
τ_{yA}	$g(\bar{d}_A)$	0.5	$[-3.7, \ 0.1]$	$\tau_{4A} = \tau_{5A} = \ldots = \tau_{I+4\ A} = \tau_A^*$, $\tau_A^* \leq \tau_J^*$	$[-5.4, \ 1.0]$	3
$g(\pi_{C_{12}})$	$g(C_{12}/R_1)$	0.0	$[-7.2, -0.6]$		$[-8.0, -0.5]$	4
$g(\pi_{M_{12}})$	$g(M_{12}/R_1)$	0.0	$[-7.2, -0.6]$		$[-8.0, -0.5]$	4
$g(S_{12})$	$g(\frac{C_{13}/\bar{c}_3}{R_1})$	0.0	$[-7.2, -0.6]$		$[-8.0, -0.5]$	4
c_{i2}			$(0.00, 0.17]$	$c_{22} = c_{32} = \ldots = c_{I2} = c_2^*$	$(0.00, 0.20]$	
c_{i3}			$(0.00, 0.67]$	$c_{13} = c_{23} = \ldots = c_{I3} = c_3^*$, $c_3^* \geq c_2^*$	$(0.00, 0.76]$	
c_{i4}			$(0.00, 0.81]$	$c_{14} = c_{24} = \ldots = c_{I4} = c_4^*$	$(0.00, 0.81]$	
c_{i5}			$(0.00, 0.81]$	$c_{15} = c_{25} = \ldots = c_{I5} = c_4^*$	$(0.00, 0.81]$	
m_{i2}			$(0.00, 0.26]$	$m_{22} = m_{32} = \ldots = m_{I2} = m_2^*$	$(0.00, 0.31]$	
m_{i3}			$(0.00, 1.00)$	$m_{13} = m_{23} = \ldots = m_{I3} = m_3^*$, $m_3^* \geq m_2^*$	$(0.00, 1.00)$	
m_{i4}			$[0.63, 1.00)$	$m_{14} = m_{24} = \ldots = m_{I4} = m_4^*$, $m_4^* \geq m_3^*$	$[0.63, 1.00)$	
d_{i1}			$[0.52, 1.00)$	$d_{21} = d_{31} = \ldots = d_{I1} = d_J^*$	$[0.50, 1.00)$	
d_{i2}			$[0.03, 0.65]$	$d_{22} = d_{32} = \ldots = d_{I2} = d_A^*$, $d_A^* \leq d_J^*$	$[0.01, 0.93]$	
$d_{ia},\ a \geq 3$			$[0.03, 0.65]$	$d_{1a} = d_{2a} = \ldots = d_{Ia} = d_A^*$	$[0.01, 0.93]$	
$\pi_{C_{12}}$			$(0.00, 0.42]$		$(0.00, 0.46]$	
$\pi_{M_{12}}$			$(0.00, 0.42]$		$(0.00, 0.46]$	
S_{12}			$(0.00, 0.42]$		$(0.00, 0.46]$	

Table A.2 Model SCR-2 parameter starting values and estimation specifications (upper portion), and translation of specifications to vital rate scale (lower portion).

	Starting Value				Estimation	
Parameter	Mean	CV	Range	Additional constraints	Bounds	Phase
η_y	$g(\bar{c}_4)$	0.4	$[-7.0, \quad 0.5]$	$\eta_3 = \eta_4 = \ldots = \eta_{I+5} = \eta^*$	$[-7.0, \quad 0.5]$	1
λ_2	$g(\bar{c}_2) - \eta^*$	0.4	$[-6.4, -2.8]$	$\lambda_2 \geq -9 - \eta^*$	$[-7.5, -2.0]$	1
λ_3	$g(\bar{c}_3) - \eta^*$	0.4	$[-6.4, -0.5]$	$\lambda_3 \geq -8 - \eta^*$, $\lambda_3 \geq \lambda_2$	$[-7.5, -0.1]$	2
ζ_i	0	0.0	$[\ 0.0, \quad 0.0]$		$[-7.0, \quad 7.0]$	3
δ_2	$g(\bar{m}_2)$	0.4	$[-7.9, -1.5]$		$[-8.0, -1.0]$	3
δ_3	$g(\bar{m}_3) - \delta_2$	0.4	$[\ 0.7, \quad 9.0]$	$\delta_3 \leq 2 - \delta_2$	$[\ 0.2, \quad 9.0]$	3
ψ	$g(\bar{m}_4)$	0.4	$[\ 0.0, \quad 1.7]$	$\psi \geq \delta_2 + \delta_3$	$[\ 0.0, \quad 2.0]$	1
τ_{yJ}	$g(\bar{d}_J)$	0.4	$[-0.3, \quad 1.8]$	$\tau_{2J} = \tau_{3J} = \ldots = \tau_{I+1\ J} = \tau_J^*$	$[-0.4, \quad 2.0]$	3
τ_{yA}	$g(\bar{d}_A)$	0.5	$[-3.7, \quad 0.1]$	$\tau_{3A} = \tau_{4A} = \ldots = \tau_{I+4\ A} = \tau_A^*$, $\tau_A^* \leq \tau_J^*$	$[-5.4, \quad 1.0]$	3
c_{i2}			$(0.00, 0.10]$	$c_{12} = c_{22} = \ldots = c_{I2} = c_2^*$	$(0.00, 0.20]$	
c_{i3}			$(0.00, 0.63]$	$c_{13} = c_{23} = \ldots = c_{I3} = c_3^*$, $c_3^* \geq c_2^*$	$(0.00, 0.76]$	
c_{i4}			$(0.00, 0.81]$	$c_{14} = c_{24} = \ldots = c_{I4} = c_4^*$	$(0.00, 0.81]$	
c_{i5}			$(0.00, 0.81]$	$c_{15} = c_{25} = \ldots = c_{I5} = c_4^*$	$(0.00, 0.81]$	
m_{12}			$(0.00, 0.20]$	$m_{12} = m_2^*$	$(0.00, 0.31]$	
$m_{i2},\ _{i \geq 2}$			$(0.00, 0.20]$	$m_{22} = m_{32} = \ldots = m_{I2} = m_2^*$	$(0.00, 1.00)$	
m_{13}			$(0.00, 1.00)$	$m_{13} = m_3^*$	$(0.00, 1.00)$	
$m_{i3},\ _{i \geq 2}$			$(0.00, 1.00)$	$m_{23} = m_{33} = \ldots = m_{I3} = m_3^*$	$(0.00, 1.00)$	
m_{i4}			$[0.63, 1.00)$	$m_{14} = m_{24} = \ldots = m_{I4} = m_4^*$, $m_4^* \geq m_3^*$	$[0.63, 1.00)$	
d_{i1}			$[0.52, 1.00)$	$d_{11} = d_{21} = \ldots = d_{I1} = d_J^*$	$[0.50, 1.00)$	
$d_{ia},\ _{a \geq 2}$			$[0.03, 0.65]$	$d_{1a} = d_{2a} = \ldots = d_{Ia} = d_A^*$, $d_A^* \leq d_J^*$	$[0.01, 0.93]$	

Table A.3 Model SCR-3 parameter starting values and estimation specifications (upper portion), and translation of specifications to vital rate scale (lower portion).

	Starting Value				Estimation	
Parameter	Mean	CV	Range	Additional constraints	Bounds	Phase
η_y	$g(\bar{c}_4)$	0.4	$[-7.0, \quad 0.5]$	$\eta_3 = \eta_4 = \ldots = \eta_{I+5} = \eta^*$	$[-7.0, \quad 0.5]$	1
λ_2	$g(\bar{c}_2) - \eta^*$	0.4	$[-7.0, -2.6]$	$\lambda_2 \geq -9 - \eta^*$	$[-7.5, -2.0]$	1
λ_3	$g(\bar{c}_3) - \eta^*$	0.4	$[-7.0, -0.4]$	$\lambda_3 \geq -8 - \eta^*$, $\lambda_3 \geq \lambda_2$	$[-7.5, -0.1]$	1
ϕ_{i2}	$g(\bar{m}_2)$	0.4	$[-7.9, -1.3]$	$\phi_{12} = \phi_{22} = \ldots = \phi_{I2} = \phi_2^*$	$[-8.0, -1.0]$	2
ϕ_{i3}	$g(\bar{m}_3)$	0.4	$[-7.8, \quad 1.6]$	$\phi_{13} = \phi_{23} = \ldots = \phi_{I3} = \phi_3^*$, $\phi_3^* \geq \phi_2^*$	$[-7.8, \quad 2.0]$	2
ψ	$g(\bar{m}_4)$	0.4	$[\quad 0.0, \quad 1.6]$	$\psi \geq \phi_3^*$	$[\quad 0.0, \quad 2.0]$	1
$\xi_{y,\ y \leq I+3}$	0	0.0	$[\quad 0.0, \quad 0.0]$		$[-5.0, \quad 5.0]$	2
ξ_{I+4}	0	0.0	$[\quad 0.0, \quad 0.0]$		$[-2.0, \quad 2.0]$	2
γ_J	$g(\bar{d}_J)$	0.4	$[-0.3, \quad 1.7]$		$[-0.4, \quad 2.0]$	2
γ_A	$g(\bar{d}_A) - \gamma_J$	0.5	$[-4.9, -1.5]$	$-3.7 - \gamma_J \leq \gamma_A \leq 0.1 - \gamma_J$	$[-5.0, -1.0]$	2
c_{i2}			$(0.00, 0.12]$	$c_{12} = c_{22} = \ldots = c_{I2} = c_2^*$	$(0.00, 0.20]$	
c_{i3}			$(0.00, 0.67]$	$c_{13} = c_{23} = \ldots = c_{I3} = c_3^*$, $c_3^* \geq c_2^*$	$(0.00, 0.76]$	
c_{i4}			$(0.00, 0.81]$	$c_{14} = c_{24} = \ldots = c_{I4} = c_4^*$	$(0.00, 0.81]$	
c_{i5}			$(0.00, 0.81]$	$c_{15} = c_{25} = \ldots = c_{I5} = c_4^*$	$(0.00, 0.81]$	
m_{i2}			$(0.00, 0.24]$	$m_{12} = m_{22} = \ldots = m_{I2} = m_2^*$	$(0.00, 0.31]$	
m_{i3}			$(0.00, 0.99]$	$m_{13} = m_{23} = \ldots = m_{I3} = m_3^*$, $m_3^* \geq m_2^*$	$(0.00, 1.00)$	
m_{i4}			$[0.63, 0.99]$	$m_{14} = m_{24} = \ldots = m_{I4} = m_4^*$, $m_4^* \geq m_3^*$	$[0.63, 1.00)$	
d_{11}			$[0.52, 1.00)$	$d_{11} = d_J^*$	$[0.50, 1.00)$	
$d_{i1,\ i \geq 2}$			$[0.52, 1.00)$	$d_{21} = d_{31} = \ldots = d_{I1} = d_J^*$	$[0.01, 1.00)$	
$d_{1a,\ a \geq 2}$			$[0.03, 0.65]$	$d_{1a} = d_A^*$	$[0.01, 0.93]$	
$d_{ia,\ i \geq 2, a \geq 2}$			$[0.03, 0.65]$	$d_{2a} = d_{3a} = \ldots = d_{Ia} = d_A^*$	$(0.00, 1.00)$	

Table A.4 Model SCR-4 parameter starting values and estimation specifications (upper portion), and translation of specifications to vital rate scale (lower portion).

	Starting Value				Estimation	
Parameter	Mean	CV	Range	Additional constraints	Bounds	Phase
η_y	$g(\bar{c}_4)$	0.4	$[-7.0, \quad 0.5]$	$\eta_3 = \eta_4 = \ldots = \eta_{I+5} = \eta^*$	$[-7.0, \quad 0.5]$	1
λ_2	$g(\bar{c}_2) - \eta^*$	0.4	$[-6.7, -2.2]$	$\lambda_2 \geq -9 - \eta^*$	$[-7.5, -2.0]$	1
λ_3	$g(\bar{c}_3) - \eta^*$	0.4	$[-6.7, -0.4]$	$\lambda_3 \geq -8 - \eta^*$, $\lambda_3 \geq \lambda_2$	$[-7.5, -0.1]$	1
ζ_i	0	0.0	$[\ 0.0, \quad 0.0]$		$[-7.0, \quad 7.0]$	2
δ_2	$g(\bar{m}_2)$	0.4	$[-7.9, -1.4]$		$[-8.0, -1.0]$	2
δ_3	$g(\bar{m}_3) - \delta_2$	0.4	$[\ 0.5, \quad 9.0]$	$\delta_3 \leq 2 - \delta_2$	$[\ 0.2, \quad 9.0]$	2
ψ	$g(\bar{m}_4)$	0.4	$[\ 0.0, \quad 1.6]$	$\psi \geq \delta_2 + \delta_3$	$[\ 0.0, \quad 2.0]$	1
$\xi_y,\ _{y \leq I+3}$	0	0.0	$[\ 0.0, \quad 0.0]$		$[-5.0, \quad 5.0]$	4
ξ_{I+4}	0	0.0	$[\ 0.0, \quad 0.0]$		$[-2.0, \quad 2.0]$	4
γ_J	$g(\bar{d}_J)$	0.4	$[-0.3, \quad 1.9]$		$[-0.4, \quad 2.0]$	3
γ_A	$g(\bar{d}_A) - \gamma_J$	0.5	$[-4.9, -1.1]$	$-3.7 - \gamma_J \leq \gamma_A \leq 0.1 - \gamma_J$	$[-5.0, -1.0]$	3
c_{i2}			$(0.00, 0.17]$	$c_{12} = c_{22} = \ldots = c_{I2} = c_2^*$	$(0.00, 0.20]$	
c_{i3}			$(0.00, 0.67]$	$c_{13} = c_{23} = \ldots = c_{I3} = c_3^*$, $c_3^* \geq c_2^*$	$(0.00, 0.76]$	
c_{i4}			$(0.00, 0.81]$	$c_{14} = c_{24} = \ldots = c_{I4} = c_4^*$	$(0.00, 0.81]$	
c_{i5}			$(0.00, 0.81]$	$c_{15} = c_{25} = \ldots = c_{I5} = c_4^*$	$(0.00, 0.81]$	
m_{12}			$(0.00, 0.22]$	$m_{12} = m_2^*$	$(0.00, 0.31]$	
$m_{i2},\ _{i \geq 2}$			$(0.00, 0.22]$	$m_{22} = m_{32} = \ldots = m_{I2} = m_2^*$	$(0.00, 1.00)$	
m_{13}			$(0.00, 1.00)$	$m_{13} = m_3^*$	$(0.00, 1.00)$	
$m_{i3},\ _{i \geq 2}$			$(0.00, 1.00)$	$m_{23} = m_{33} = \ldots = m_{I3} = m_3^*$	$(0.00, 1.00)$	
m_{i4}			$[0.63, 1.00)$	$m_{14} = m_{24} = \ldots = m_{I4} = m_4^*$, $m_4^* \geq m_3^*$	$[0.63, 1.00)$	
d_{11}			$[0.52, 1.00)$	$d_{11} = d_J^*$	$[0.50, 1.00)$	
$d_{i1},\ _{i \geq 2}$			$[0.52, 1.00)$	$d_{21} = d_{31} = \ldots = d_{I1} = d_J^*$	$[0.01, 1.00)$	
$d_{1a},\ _{a \geq 2}$			$[0.03, 0.65]$	$d_{1a} = d_A^*$	$[0.01, 0.93]$	
$d_{ia},\ _{i \geq 2, a \geq 2}$			$[0.03, 0.65]$	$d_{2a} = d_{3a} = \ldots = d_{Ia} = d_A^*$	$(0.00, 1.00)$	

Table A.5 Convergence performance of SCR models. For each model and generating rate set, the frequency of outcomes over the 100 attempted fittings to a dataset (averaged across the 100 independent datasets) is listed. "Convergence criterion met" outcome includes both global and local minima. For further definition of outcomes see text.

		Generating rate set			
Model	Outcome	Con.2	Add.2	Var.2	Var.4
SCR-1	Failed	0.00	0.05	0.01	0.00
	Non-positive-definite Hessian	0.02	0.00	0.00	0.00
	Convergence criterion not met	1.12	24.48	1.38	0.64
	Convergence criterion met	98.86	75.47	98.61	99.36
	Local minima	0.03	0.00	0.00	0.00
SCR-2	Failed	0.00	0.20	0.04	0.08
	Non-positive-definite Hessian	0.01	0.09	0.14	0.01
	Convergence criterion not met	2.45	35.49	2.47	1.67
	Convergence criterion met	97.54	64.22	97.35	98.24
	Local minima	0.01	0.01	0.00	0.01
SCR-3	Failed	0.06	0.12	0.35	0.39
	Non-positive-definite Hessian	0.05	0.03	0.01	0.00
	Convergence criterion not met	0.53	22.11	1.27	0.29
	Convergence criterion met	99.36	77.74	98.37	99.32
	Local minima	0.20	0.15	0.39	0.38
SCR-4	Failed	0.00	0.00	0.12	0.67
	Non-positive-definite Hessian	0.00	0.00	0.00	0.92
	Convergence criterion not met	4.82	56.13	11.38	3.73
	Convergence criterion met	95.18	43.87	88.50	94.68
	Local minima	0.01	0.00	0.01	0.04